MARITIME TRANSPORTATION RESEARCH AND EDUCATION CENTER
TIER 1 UNIVERSITY TRANSPORTATION CENTER
U.S. DEPARTMENT OF TRANSPORTATION

Development of Rapid Setting Soil-Cement Mixture Designs and Performance Testing
September 2021-December 2023
Cameron D. Murray, Ph.D., P.E., Associate Professor (cdmurray@uark.edu)
Michelle Barry, Ph.D., P.E., Associate Professor (mlbernha@uark.edu)
Mariel Mayori, G.R.A. (mmayori@uark.edu)
Edgar Ortega, G.R.A. (eo009@uark.edu)
University of Arkansas

FINAL RESEARCH REPORT
Prepared for:
Maritime Transportation Research and Education Center

University of Arkansas
4190 Bell Engineering Center
Fayetteville, AR 72701
479-575-6021

ACKNOWLEDGEMENT

PROJECT DESCRIPTION

Flooding in the past few years in the U.S. has shown the concerning condition of the country´s waterway systems and the great economic impact that arises from the repair costs associated with damage to such structures, as well as the disruptions caused by their closure during downtime for repairs. Levee failures not only disrupt navigable waterways, but they can also impact rail and truck transportation. Additionally, floods can result in damage to other soil structures impacting transportation and the movement of goods including riverbanks, dams, and highway embankments. Several of these levee failures and failures of other soil-based infrastructure are due to instabilities caused by internal and overtopping erosion. Even though there are existing flood-fighting methods such as sandbagging, sand boil ringing, and tarping exposed soil, most are temporary treatments and the levees eventually require repair. Usually, the repairs require long downtimes that are difficult to carry out during flood season, and they can be quite expensive. Therefore, fast-setting soil-cement could be a cheaper and more effective alternative for short-term repair during flood season, as well as long-term repairs of the levee. Rapid setting soil-cement can utilize onsite soils, which reduces transportation and labor costs and it can be used to create a strong surface armoring in a matter or hours or even minutes. Conventional portland cement-based soil-cement has been commonly used as the repair method for waterway structures for decades, but the rapid setting time, strength gain, and reduced shrinkage of rapid-set cements such as belite calcium sulfoaluminate (BCSA) make it a promising alternative to conventional cement for such flood repair efforts. This project studies the effectiveness of various proportions of BCSA soil-cement mixtures by measuring their early age compressive strength and their performance under simulations of piping conditions through the Hole Erosion Test.

Research Significance

In March 2021, the most recent infrastructure report card from the American Society of Civil Engineers (ASCE) was released. This report assigned a D grade to crucial U.S. flood control infrastructure, dams, and levees. ASCE reported that the estimated cost to rehabilitate all U.S. dams was $93.6 billion. Levee repairs were estimated at $1 billion. However, they estimated that levees prevented almost $350 billion in flood damage from October 2018 to September 2019. Furthermore, at least 17 million people in the country live or work behind a levee, and levees protect $2.3 trillion in property, making the condition of such structures a critical concern [1].

Soil-cement has been used for repair in waterway structure applications; however typical soil-cement mixtures require long times to achieve full strength and durability. The financial implications of this downtime encompass not only the expenses associated with repairs and dewatering but also the economic consequences stemming from potential road or waterway closures, leading to delays and business losses.

Rapid-setting soil-cement has many potential applications including rapid levee or dam repair, channel repairs, stabilizing foundation systems and excavations, and deep soil mixing ground improvement. The rapid strength gain and underwater capabilities of a belitic calcium sulfoaluminate (BCSA) soil-cement mean many of these applications could be deployed quickly before additional storms damage the maritime infrastructure further. More importantly, they can be used for rapid repairs of levee and dam surfaces even during flooding events and as a part of flood fighting efforts. A rapid-setting material such as BCSA cement which sets quickly, gains strength rapidly, and exhibits minimal shrinkage is an excellent choice for repair purposes [2]. BCSA cement also represents a more sustainable alternative to conventional cement due to its lower carbon footprint during production.

Results from previous research performed at the University of Arkansas showed that 7.5 percent moisture content BCSA soil-cement mixtures can achieve strengths of 131 psi in compression after one hour of curing compared to only 50 psi reported from the PC soil-cement samples [3]. However, the full range of properties of BCSA-based soil-cement mixtures is unknown. This investigation focused on generating experimental data to guide the proper dosage of BCSA in soil-cement mixtures, evaluate their setting times, and examine their ability to reduce soil erodibility. To investigate the susceptibility of soil-cement mixtures to erosion, hole erosion tests (HET) were conducted using a newly developed system, based on the original method proposed by engineers Wan and Fell at the University of New South Wales in 2002. This test aimed to replicate a form of internal erosion known as piping which can lead to internal instability of the levee and failure. Baseline erodibility was also determined from HET results on uncemented soil samples.

The findings show that even small amounts of BCSA cement (1-3 percent by weight) can significantly reduce the erodibility of a range of soil types. Soils that could not even be tested in the HET due to the hole collapsing were able to resist erosion after only 1 hour with only 1 percent cement by weight used. While more research is needed to fully document the capabilities of BCSA soil-cement mixtures in the field, the laboratory study presented herein demonstrates the exciting potential of these materials.

LITERATURE REVIEW

Soil Stabilization: Definition, Importance and History

Soil structures such as foundations, levees, dams, and canals are frequently used in the context of waterways and water retaining structures. To improve the permeability and strength of soils, soil stabilization is often used. Soil stabilization is the process of modifying the physical properties of soil with an additive to enhance its characteristics and overall performance. This additive could be a specialized soil, cementing material, or chemical substance to augment the natural soil, aiming to improve one or more of its properties [4].

There are two main types of stabilization, chemical or mechanical, which can improve the engineering properties of soil according to ASTM D-18 [5]. Mechanical stabilization may refer to techniques like soil nails, geotextiles, or mechanically stabilized earth. When it comes to chemical stabilization, there are two common agents: lime, whose solidification process is a long-term reaction that continues for years [6] and cement which reacts relatively more quickly but can also continue to gain strength over long time periods. Soil stabilization through the addition of cement or lime is an ancient practice. Lime stabilization was used in the construction of the pyramids of Shensi in the Tibetan Mongolian Plateau, dating back over 5,000 years. Lime was also useful to civilizations such as the Greeks and Romans to stabilize earth roads, with the application of lime in the subbase of their roads more than 2000 years ago. However, the application of lime in construction probably existed even before the construction of such roads [7].

Portland cement was patented in 1824 and it was first used as a stabilizer for soil in road construction in 1915 when a street was built in Sarasota, FL, utilizing a blend of shells, sand, and portland cement. Its notable effectiveness as a soil stabilization technique made it a popular choice for highways and it became more popular. A soil-cement base offers

consistent and durable support for pavements, preventing consolidation when subjected to traffic [8]. Soil-cement began to be used for other structures, such as dams, at this time. Some early research in soil-cement included a study that the Bureau of Reclamation performed over a span of 10 years on soil-cement in the 1950s at Bonny Dam in Colorado. The results of the investigation proved the durability of soil-cement for slope stabilization by successfully resisting freeze-thaw and wet-dry cycles. This work led to more frequent use of the material in the 1960s and 1970s. Engineers later applied soil-cement to stabilize stream banks and to prevent erosion, with successful projects in Phoenix, Tucson, and Orange County. By the early 2000s, soil-cement was in widespread use for applications such as bank stabilization due to its proven outstanding performance related to protection during floods [9]. In recent studies, there has been a focus on evaluating the soil-cement ratio through various laboratory experiments. These tests aim to determine the smallest quantity of cement needed to attain desired characteristics regarding firmness, robustness, and longevity. However, soil-cement exhibits complex behavior since it is influenced by numerous factors. These factors include the physical and chemical properties of the soil, the amount of cement used, as well as the porosity and moisture content during compaction [10]. This research focuses on soil stabilization that uses a rapid setting cement (BCSA) as the stabilizing agent. There is little to no research on this topic as of this writing.

Cement Stabilization

Cement is a versatile stabilizer for various soils. Unlike in lime stabilization, cement develops strength faster, eliminating the need for a "mellowing" period. Compaction can occur within 2 hours of mixing, although the achieved strength during compaction may be below the ultimate strength of the soil–cement sample.

The implementation of cement for soil stabilization has been successful in a variety of applications [11]. The addition of cement to the soil serves two primary purposes: 1) It fills empty voids, preventing water from entering the soil, and 2) it enhances the strength properties of the soil as the cement cures [12]; [13].

The International Committee of Large Dams (ICOLD) has defined soil-cement as a mixture of the following materials: portland cement, soil, and water, these materials are compacted, then bonded together through the hydration process, resulting in a durable material with low permeability and good wear resistance [14] It is an economical material created by compacting the mixture to high density which makes it a durable and strong alternative with a strength somewhere between compacted soil and concrete or natural rock [15].

To ensure that the desired qualities and serviceability requirements of soil-cement are met, there are four essential factors to ensure: 1. Enough cement needs to be added to the mixture [8]. 2. The appropriate quantity of water must be uniformly blended with the soil-cement mixture. 3. The soil-cement mixture needs to be compacted to an appropriate dry unit weight prior to cement hydration. 4. The soil content should not exceed 45 percent retained on a No. 4 U.S. Series sieve, nor should any portion exceed 2 inches in size [16], [17].

According to Choi and Hansen, the soil used in soil-cement should have a fines content ranging from 5 to 35 percent with a maximum plasticity index of 8, but more than 35 percent percent fines are allowed if the fines are non-plastic [18].

Table 1 is provided in the "Soil Cement Laboratory Handbook", 1992 by PCA [16] and it contains the recommended portland cement content for different soil groups of various AASHTO classifications, specifically those soil groups of class "A". Recommended values are meant to be used for initial mixture design, since the required or suitable cement content

will be project-based and should be confirmed with laboratory testing once more information is available. It is noted that these guidelines are for roadway applications and that cement content may vary for other applications.

Table 1. Common percentage of cement required for class category "A" soils in AASTHO classification[16].

AASHTO Soil Group	Common cement content required by weight of soil [%]
A-1 a	3 to 5
A-1 b	5 to 8
A-2	5 to 9
A-3	7 to 11
A-4	7 to 12
A-5	8 to 13
A-6	9 to 15
A-7	10 to 16

Mixing, Placing and Compacting Soil cement:

There are two methods to mix soil cement. The central plant mixed method consists of mixing the soil-cement in an approved continuous-flow or batch-type pugmill or rotary-drum mixer until a uniform blend of soil, cement, and water is achieved. The soil-cement mixture is then transported by a covered truck Once on site, the soil-cement mixture is placed without segregation. One or more approved spreading devices can be used for even distribution. Compaction should start promptly after placement of the mixture, and the total elapsed time between water addition and compaction should not exceed 45 minutes [19], [20].

Another mixing and placement option is the mixed-in-place method. The in-place soil may need or may not need to be scarified and pulverized to the full mixing depth before cement is added, the occasions when scarification and pulverization is needed are: material's plasticity index is greater than 20, for full depth recycling of flexible pavements before the bituminous layer is added, and when slurry application is needed. Following this step, the cement is

spread uniformly followed by the application of water. The entire process of cement spreading, water application, and mixing should result in a consistent soil, cement, and water mixture throughout the full design depth and width, and as soon as the section has been mixed it proceeds to be compacted [19], [20]. During compaction, no section should remain undisturbed for over 30 minutes, and all compaction operations must conclude within 2 hours from the start of mixing. The finishing process involves protecting the applied layer and applying a sealing membrane or maintaining continuous moisture for 7 days [19].

Reinforcement and Repair of Waterway Structures Using Soil-Cement

Soil-cement has been used for embankment slope protection of water control structures such as embankments and channels. Also, soil-cement has been used as a liner for reservoirs, lakes, and landfills [18]. It is used to provide streambank protection from lateral erosion during floodings, channels linings, and prevent degradation of water control structures by building structures that raise the elevation of water surface [21].

Soil cement gained popularity after being successfully applied in water resources projects of Tucson, Arizona floods in 1978 and 1983, where reinforcement of structures such as slope and bank protection were developed as part of their efforts to prevent damages for future floodings [22]. Despite water overtopping the bank protection, soil stabilization saved millions of dollars in property damage. As a result, Tucson increased the use of soil-cement for these kinds of projects, and later, in 2002 Los Angeles County, California, formally adopted soil-cement as an acceptable material for bank stabilization in the county. The soil-cement is usually placed in a stair step design with minimum compressive strength of 600 to 750 psi to successfully resist the force of stormwater flows for velocities up to 20 ft/sec [21].

Even though the strength requirements will vary according to climate conditions, the frequency of use among other specific characteristics about the project. The Portland Cement

Association has stated that generally, for a 7-day test on compressive strength test, a soil-cement mixture that reports around 300 psi will pass the wet-dry and freeze-thaw test satisfactorily [23]. Therefore, for water resources applications, the 7-day saturated specimens will be generally within the range of 300 to 800 psi. However, typically, the required minimum in-place unconfined compressive strength for water resources applications at 7 days, period chosen based on the early strength measurements before the material under consideration was covered by additional layers of soil-cement, are 500 psi for liners, 600 psi for bank protection, 1000 psi for grade control structures to produce adequate hardened soil-cement [24];[25];[26].

Given that recent flooding events in Oklahoma, Missouri, Illinois, and Arkansas have tested the nation's waterway systems and highlighted their vulnerability and the impact that damage to these systems can have on the transportation system, addressing defective or damaged levees is an important goal. Levee failures not only disrupt navigable waterways, but they are capable of impacting rail and truck transportation. Additionally, floods can result in damage to several other soil structures impacting transportation and the movement of goods including riverbanks, dams, and highway embankments. There is a need for faster and more non-invasive mitigation strategies to avoid larger failures and keep the closure time of such structures at its minimum. A fast-setting soil-cement mixture capable of reducing erosion would also reduce downtime, reduce or eliminate the need for de-watering, and rapidly address deficiencies in waterway structures. Such a material would combine the traditional benefits of soil-cements outlined in this literature review with the added benefit of setting speed.

BCSA Cement

Belitic calcium sulfoaluminate (BCSA) cement is a rapid setting, low shrinkage cement originated from the CSA family of cements which have their origins in research conducted by Professor Alexander Klein in the 1960s. He initially focused on using a CSA additive to counteract the drying shrinkage from portland cement.

CSA cement production requires lower kiln temperatures compared to portland cement, thereby reducing the environmental impact when compared to portland cement. Kiln temperatures of about 1250ºC are required for BCSA vs 1500 ºC for portland cement. This decrease in sintering temperature makes the CSA cement a greener alternative since the carbon dioxide emissions associated with its production are significantly reduced [27]. There is a growing concern about the environmental impact of portland cement manufacturing. According to certain estimates, the cement industry alone may have accounted for as much as 5 percent of the overall CO2 emissions worldwide in 1999 [28]. For this reason, CSA-based cements such as BCSA cement may be a promising alternative moving forward.

Most CSA cements are characterized by their high early strength, rapid setting time, excellent durability, and significantly reduced carbon footprint [29]. BCSA cement is a variant of CSA discovered by Borje Ost in 1975. Ost suggested formulating a CSA cement with a substantial amount of belite (C_3S), making it possible to create a cement (BCSA) that is a standalone cement with good later age strength gain. BCSA cement grew in production and its use has spread in the United States since the 1980s [29].

Research has previously been performed testing the benefits of using BCSA cement for underwater applications. It was found that BCSA was able to achieve about 28 MPa in 3

hours or less. [3]. Therefore, the use of this cement in the soil-cement mixtures could help to reduce the repair time for maritime structures, eliminating the need for dewatering.

The initial setting time of BCSA cement can be as little as 10-20 minutes and compressive strengths of about 4000 psi can be achieved within as little as 2-4 hours when retarder is used [30]. The rapid rate of strength gain during the initial stages of concrete hydration is primarily attributed to the creation of ettringite, whereas the enhancement of strength in later stages is a result of the gradual hydration of belite [31].

To prevent self-desiccation and allow the reaction to take place, it is essential to have a sufficient water supply when using BCSA cement. Due to its rapid strength gain, the application of BCSA cement is usually restricted to scenarios where there is a need for expedited construction [27]. Consequently, even though the rapid setting time and strength development of BCSA is advantageous and attractive, increasing the working time is crucial for most purposes, and various substances have been demonstrated to effectively delay or retard its hydration process [32]. Citric acid has been the most used retarder.

BCSA cement could be applied to make fast-setting soil cement. Repair applications or underwater placements would be ideal for such a material. Unfortunately, little to no guidance exists for applying this specific type of CSA cement to soil mixtures. The few research articles documented studied the improvement of mechanical properties of expansive soils when adding CSA. Similar to the tests performed at the University of Arkansas, the paper mentions that their soils were dried before being used in order to be more precise with their target moisture contents. They tested percentages of commercially available CSA cement at 1, 3, 5, 7 and 10 percent by dry weight of soil at 2 percent wetter than the optimum moisture content of the soils alone. Compaction was carried out using a conventional proctor test procedure and unconfined compressive strength testing was employed after curing times

of 1, 7, 14 and 28 days at 3/64 in. per min until 15 percent strain. No retarder was mentioned in either of these studies. Among their findings, they observed that with 1 percent cement content, the strength was low at all ages at an average of 43 psi. They also found that for 1 percent, and 3 percent cement content the improvement of the soil was more considerable for ages of 1 to 7 days, but no improvement was found at older ages. They mentioned that their error margins were greater for the mixes with 7 and 10 percent cement content, which can be potentially due to an uneven distribution of water to CSA cement particles [33].

This article also studied sands treated with CSA cements tested for UCS 1, 7, and 28 days after curing, and stated that increasing cement content led to higher strength values, but the article emphasizes the effect of fines contents in the mixture. Even though the study tried to increase strength by simultaneously adding industrial grade kaolin, they found that the compressive strength of the mixes benefited when the amount of fines was increased [34].

Citric acid

Citric acid is a commonly used set retarder for BCSA cement [56]. While other retarders may be used, citric acid has been commonly used in research and practice since is a naturally occurring acid with diverse applications in various industries including food, beverage, pharmaceutical, cosmetic, agricultural, and chemical sectors. Utilizing citric acid as a retarder offers an eco-friendly option [35].

Little or no research has focused on BCSA soil-cement mixtures and the impact of incorporating citric acid in the mix. It is essential to understand the correct retarder dosage required for appropriate setting time to make BCSA soil-cement practical to use. Characterizing the working time and strength at different citric acid dosages is one of the

main goals of the current research. This knowledge is needed to understand how to effectively place and consolidate fast-setting soil-cement mixtures in the field.

Burris and Kurtis performed studies about the impact of varying citric acid dosages on the properties of CSA pastes and mortars incorporating two commercially accessible CSA cements. Their findings revealed that citric acid serves as a proficient retarder, delaying the hydration process, affecting both the initial and final setting times, as well as prolonging the duration between these two stages as the dosage increases. The research established a correlation between the setting time, particularly the final setting time, and the peak rate of heat reported by the samples [36]. The correlation between the quantity of citric acid utilized and the initial setting time is evident, the studies conducted by Soriano showed a linear trend between the citric acid dosage and the setting time. Moreover, the dosage has been proven to cause a direct impact on the difference between the initial and final setting times, with higher amounts leading to an increased difference, in a linear relationship. It was also found that the addition of citric acid also influences additional properties such as the viscosity of the mixture and the internal reaction temperature [37].

Soil Waterway Structures and Their Erosion Mechanisms

Embankments, in general terms, refer to structures used to confine water. However, there is a distinction between embankment dams and levees based on their function. Dams are designed to hold water upstream, while levees, also known as flood protection dikes, are intended to prevent the spread of water into vulnerable areas [38]. These waterway structures are found throughout the world due to their water control function. However, the presence of water penetrating these structures can potentially lead to structural failure or catastrophic damage.

The International Commission on Large Dams (ICOLD) published a statistical analysis of dam failures containing worldwide dam failure information from 1970 to 2018 [39]. This

document presented the failure mode of embankment dams (earth fill and rock fill) and rigid dams (rigid materials such as concrete) and the primary factors contributing to substantial damage are established to be structural issues and slope instability, overtopping, and seepage or internal erosion [40].

Another study developed a database of more than 1600 dam failure cases from 50 different countries around the world from a variety of sources such as ICOLD, the United States Committee on Large Dams (USCOLD), and researchers' investigations, established that 66 percent of all the failures involved earth dams which are the most common type of dam worldwide. According to US Committee on Large Dams data, at least 80 percent of the large dams in the United States are earth dams made of soil material, which is especially vulnerable to failure due to erosion [38], [41]. In 2022, Zhong et al. [42] published an article presenting a state of art review of embankment dams. The review included recorded historical failures, laboratory, and field experiments and main failure types for earthfill and rockfill dams based on 3504 cases worldwide. It is stated that overtopping along with piping erosion, which is a type of internal erosion, represents the most common failure of embankment dams. Figure 1 summarizes the types of failures from all the different sources that Zhong collected in the paper.

Earthen levees and dams can be eroded by a combination of action from wind, water, and ice. The extent of the erosion is dependent the soil material, the properties of the fluid causing the erosion, and the design of the structure[43]. The primary cause of erosion is from the movement of water [44]. This water-caused erosion can occur on the exterior or interior of the structure [45].
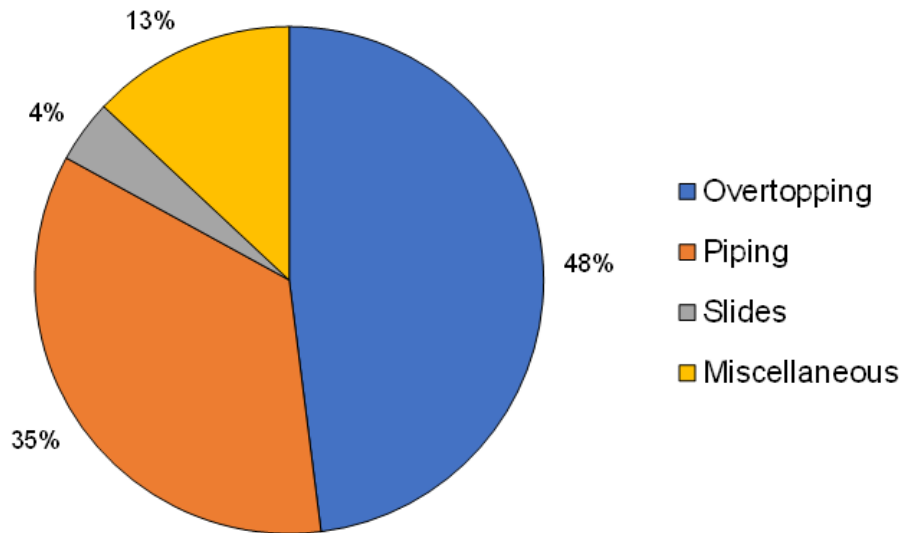
Figure 1.Typical failure modes for embankment dams [46].

Failures due to overtopping occur when water action flows on top of or around the embankment [45]. This external erosion removes the top or outer layer of the structure and reduces its longevity and strength. Three main stages of overtopping erosion have been proposed by [44]:

1. The moving water causes forces at the interface between the soil or rock.
2. The moving water reduces the normal stress at the surface of the soil or rock. This mechanism is based on energy conservation and Bernoulli's principle.
3. The combination of the eroded soil and turbulent water flow introduces cyclic loads to the soil, making erosion occur with greater ease.

Internal erosion causes soil particles to be carried away by water which has entered cracks, or voids in the soil itself [47]. This seepage of water can progressively erode the structure from within and cause a failure.

Suffusion and piping are the two fundamental types of internal erosion [48]. Both describe a mechanism by which soil particles are removed from the interior of a soil structure by moving water. However, they can be differentiated because suffusion is when smaller particles are removed from the gaps between larger particles, resulting in coarser soil particles being left behind as all fines are washed away [49] and piping refers to the creation of tunnels or pipes inside the soil structure [50]. The diameter of these "pipes" varies and can be less than an inch, up to several feet [21]. Piping can be challenging to identify externally. This makes it a risky failure type for waterway structures. The indicators of piping erosion, such as sinkholes, crest settlement, or changes in pressure, might not be visible until a failure has occurred [51].

Understanding the soil's susceptibility to erosion is a fundamental step in investigating and mitigating the significant safety risks associated with erosion on levees. Consequently, several researchers have devised various tests to examine the characteristics of external and internal erosion in soils. These same characterization methods can be used on repair materials to determine their applicability to waterway soil structures.

Erosion Devices and Testing

Multiple erosion tests can be used to quantify the erosion rate and critical shear stress. These parameters are crucial for characterizing soil properties in relation to external and internal erosion. These devices and tests can be categorized as follows [47]:

1. Flow over surface

2. Rotating cylinder

3. Jet impact

4. Flow through defect

The following sections discuss test methods that have been proposed in these categories.

1. Erosion Function Apparatus

Surface erosion in river channels or unlined canals occurs by the free flow of water on a soil surface. Testing this erosion mechanism is usually simulated by utilizing a hydraulic flume. Soil specimens are positioned on the flume bed and exposed to open channel flow. This mimics the scenario of water flowing parallel to the soil surface at specific velocities and depths [47].

In the early 1990s, the concept of the erosion function apparatus (EFA) was pioneered and established by Briaud at Texas A&M University. Originally designed for assessing the erodibility of a diverse range of soils, both cohesive and non-cohesive—including gravel, sand, clay, and silt—the EFA has become a standard tool in geotechnical engineering [43]. Soil samples are collected using (ASTM D1587) standard Shelby tubes [52] and then the tubes can be placed into the EFA and positioned with the tube and soil sample surface flush to the bottom of the flow pipe. To initiate the erosion process, water—the eroding fluid—is driven by a pump into a 3.94 ft. long rectangular cross-section pipe measuring 4 in. by 2 in. Control of the water flow velocity is facilitated by a valve, and the average water velocity is monitored through a flow meter in the flow line. The Shelby tube soil sample, positioned with one end on the bottom of a circular plate connected to a piston, is designed to be pushed upward when required [53].

2. Rotating Erosion Apparatus

Various configurations of erosion test apparatuses designed to measure the erosion resistance of cohesive soils through a rotating cylindrical fluid chamber are collectively referred to as the rotating cylinder test (RCT). In this test, a soil specimen is immersed and suspended

within a fluid filled cylindrical chamber. The chamber is then rotated in relation to the soil specimen, creating a flow around the specimen that imparts shear stress to the soil surface [47].

The test apparatus is equipped with a torque transducer at its base and a load cell to record the weight of the sample. The apparatus is also equipped with a water-cooling system to reduce the temperature for long tests (more than 72 h for rocks). The central shaft still exists; therefore, intact samples are not usable unless a center hole can be drilled through them. After the hole is drilled, the sample is oven-dried and placed in the device to saturate. During the saturation, the device applies a very small torque to the sample for at least a day to remove any loose material [54]. A downside of the method is that it has been designed specifically for testing stiff clay and resilient rock types like limestone. Additionally, intact samples prove impractical unless a center hole can be drilled through them.

3. Jet Erosion Test

Jet erosion tests simulate spillway channel erosion from a submerged jet [47]. The United States Department of Agriculture (USDA) Agricultural Research Service (ARS) Hydraulic Engineering Research Unit (HERU) in Stillwater, Oklahoma, developed the submerged jet erosion test (JET). This test can be conducted either on-site or in a laboratory, utilizing tube samples or remolded samples in compaction molds [55]. The JET apparatus is designed to impact the soil surface with a submerged jet generated by a 0.25 in. diameter nozzle initially positioned between 6 and 30 nozzle diameters from the soil surface. While the starting nozzle position and test head can be adjusted to vary the stress on the soil sample, once selected, these parameters are typically kept constant throughout the test. The jet can also be angled if desired. The scour of the soil surface beneath the jet is measured over time (usually up to 2 hours) using a point gauge aligned with the jet's axis [55].

The primary limitations of this test include the inability to test particles larger than 1.20 in. due to the small sample size. Moreover, coarse-grained soils, such as noncohesive sand and gravel, tend to fall back into the open hole during the jet erosion process, casting doubt on the accuracy of the readings.

4. Hole Erosion Test and Slot Erosion Test

Categorized as internal erosion tests, flow through defect erosion tests replicate conditions along a crack or any flow path within an earthen structure. These tests use an undisturbed or reconstituted soil specimen with a preformed defect introduced before testing. The specimen undergoes controlled pressure flow, and hydraulic conditions are monitored to assess shear stress and erosion rate [47]. The two main varieties of this test are the hole erosion test and the slot erosion test.

The slot erosion test (SET), introduced by Wan and Fell in Australia in 2002 involves drilling a 0.1 in. wide, 0.39 in, slot at the surface of a 3.28 ft. long rectangular soil sample [43]. Water is then introduced into the slot at a specified velocity, and the erosion rate is determined by recording the rate of mass removal per unit area over time. The construction cost of the device typically ranges from $20,000 to $35,000.

The hole erosion test (HET) has been developed to investigate piping erosion in earthen structures [51]. In the HET, a soil sample containing a preformed axial hole is subjected to controlled flow conditions, and by measuring the hydraulic gradient and flow rate, it is possible to indirectly determine the rate at which the simulated soil pipe expands [40]. The HET evolved from its predecessor, the pinhole erosion test, and is credited to Robin Fell in Australia [49]. This test involves drilling a 0.24 in. diameter hole through a compacted soil sample made using a standard 4in. diameter proctor mold and directing water to flow through

the hole at a selected velocity. The apparatus typically allows for variable heads ranging from

0.14 psi to 1.14 psi, and the flow is regulated using a valve. The erosion rate is then recorded

as the rate of mass removal per unit area over time. Upon the detection of erosion, the test is

sustained at a consistent hydraulic load for a duration of up to 45 minutes or until flow

stability is achieved. Various parameters, such as flow measurements, differential pressure,

and the initial and final diameter of the erosion hole, are utilized to determine the applied

shear stress and erosion rate [55].

As mentioned previously, this research project focused on the HET to measure the piping

resistance of fast setting soil cement. Because of this, more detail on the HET device and the

interpretation of its results is provided.

The underlying theory for deriving the hydraulic shear stress is based on the equilibrium of

forces in the eroding fluid body along a differential length of an axial circular borehole. Such

equilibrium is expressed by equation (1) [47]:

$$F_R = F_F: \tau P \, dL = A \, dp \qquad\qquad (1)$$

where:

F_R= retaining force, lb.

F_F= forcing force, lb.

τ= hydraulic shear stress along wetted area, lb/ft^2.

P= wet perimeter, ft.

L= length of axial hole, ft.

A= cross-sectional area of axial hole, ft^2.

p= fluid pressure, lb/ft^2.

Equation (2) allows for the expression of the pressure differential, dp, along a length differential, dL, in a uniform circular cross-section with fully developed flow. According to Luthi [47], this pressure differential can be related to the friction head loss, h_f:

$$dp\,(dL) = \rho g\,dh_f \tag{2}$$

where:

ρg = specific weight of eroding fluid, lb/ft^3

Combining equation (1) with (2) gives equation 3 as follows:

$$\tau = \frac{A}{P}\frac{dp}{dL} = \rho_w g\,\frac{A}{P}\frac{dh_f}{dL} = \rho_w g\,\frac{\phi}{4}\frac{dh_f}{dL} \tag{3}$$

where:

ρ_w = density of water as eroding fluid, lb/ft^2

g = acceleration of gravity, 32.2 ft/s^2.

Equation (3) introduces the term $\frac{A}{P}$, which is referred to as the hydraulic radius. In the case of a circular ccross-section this term is equivalent to $\frac{\phi}{4}$. Equation (3) applies to the overall length of the soil specimen and is based on the following assumptions according to the report by Wan and Fell [49]:

1. Negligible flow through the soil matrix.

2. Shear strength is provided solely by the soil surface surrounding the preformed hole.

3. Negligible energy losses due to the entry and exit of the erosion fluid into the preformed hole.

4. The soil sample exhibits a uniform circular cross-section.

5. A fully developed flow profile exists within the preformed hole along the soil sample.

6. The differential pressure or hydraulic head difference, Δh, across the soil sample equals the total frictional head loss, h_f.

The shear stress within the soil sample is directly proportional to the frictional head loss experienced along its length, considering a specific diameter. The frictional head loss measures the energy dissipation due to flow resistance and is indicated by the hydraulic gradient across the soil sample [48]. Equation (4) defines the shear stress, and (5) the hydraulic gradient as:

$$\tau_t = \rho_w g s_t \frac{\phi_t}{4} \tag{4}$$

$$s_t = \frac{\Delta h}{L} = \frac{h_u - h_d}{L} \tag{5}$$

where:

τ_t= estimated wall shear stress along axial hole, lb/ft^2 on the surface of the pre-formed hole at the time t.

s_t= hydraulic gradient across the soil specimen at the time t.

ϕ_t= estimated mean diameter of axial hole at the time t.

Δh= diferential pressure, ft.

h_u= measured upstream sidewall hydraulic head, ft.

h_d= measured downstream sidewall hydraulic head, ft.

L= length of axial hole, ft.

Equation (6) expresses the erosion rate per unit area of the hole at a given time, t, as described by Wan and Fell [48], [49]:

$$\dot{\varepsilon}_t = \frac{\rho_d}{2} \frac{d\phi_t}{dt} \tag{6}$$

where:

ρ_d = dry density of the soil, lb/ft^3.

$\dot{\varepsilon}_t$ = erosion rate at the time t, lb/s/ft^2.

The diameter, ϕ_t, can be estimated using equation (7) and (8):

$$\phi_t = \left(\frac{16Q_t f_{Lt}}{\pi \rho_w g s_t}\right)^{1/3} \tag{7}$$

$$\phi_t = \left(\frac{64Q_t^2 f_{Tt}}{\pi^2 \rho_w g s_t}\right)^{1/5} \tag{8}$$

where:

Q_t = flow rate, ft^3/s. At the time t.

f_{Lt} = friction factor for laminar flow, lb/ft^2/s.

f_{Tt} = friction factor for turbulent flow, lb/ft^3.

According to the procedure initially proposed by Wan and Fell [48], the HET involves measuring the differential pressure, Δh, and flow rate, Q, at selected time intervals. The initial and final diameters of the test sample are known, with the initial diameter set at 0.24 in. at the beginning of the test and the final diameter measured after the test is completed. By utilizing these variables, the friction factors at the start and end of the test can be determined, assuming a linear variation over time. From this information, the diameter, ϕ_t, and the rate of change, $\frac{d\phi_t}{dt}$, can be obtained to calculate the hydraulic shear stress along the preformed orifice, τ_t, and the erosion rate, $\dot{\varepsilon}_t$, using equations (4) and (6) respectively. Once $\dot{\varepsilon}_t$ is plotted against τ_t, the upstream part of the graph can be approximated by a straight line of best fit.

The value of the soil erosion coefficient, denoted as C_e by Wan and Fell [48], can be obtained from the slope of the straight line. This coefficient is used to determine the erosion rate index, defined in equation (9) as:

$$I = -\log{(C_e)} \tag{9}$$

where:

C_e = coefficient of soil erosion, s/m.

I = erosion rate index, with an order of magnitude in the range of 0 to 6. Table 2 presents a classification of soils, proposed by Wan and Fell (2002), based on the erosion rate index.

Table 2. Classification of soils based on the erosion rate index proposed by Wan and Fell (2002)

Group Number	Erosion Rate Index	Description
1	<2	Extremely rapid
2	2-3	Very rapid
3	3-4	Moderately rapid
4	4-5	Moderately slow
5	5-6	Very slow
6	>6	Extremely slow

Several modifications of the original HET have been developed since its inception. Some of these modifications are described here in chronological order to provide context for the modified device used in this study. More details on the development and operation of the University of Arkansas (UARK) system are given in the chapter on Experimental Procedures.

Lim (2006), University of New South Wales (UNSW), Australia

After the development of the HET, extensive tests were conducted at the geotechnical laboratory of UNSW in the context of embankment dam projects. While most tests yielded consistent and stable results in measuring erosion rates, certain deficiencies were observed, raising concerns about the representativeness of the test. These deficiencies included [56]:

1. Delay in erosion caused by the smearing effect of electric drilling used in forming the hole or the necking of certain parts of the erosion channel, leading to a smaller flow rate compared to the average hole diameter and channel length.

2. Slaking in the upstream and downstream faces of unsaturated soil samples, resulting in challenges in estimating the averaged hole diameter. Slaking also posed difficulties in estimating hydraulic shear stress due to the reduced channel length.

To address the delay in erosion, a modified procedure was proposed for the analysis of HET data. This procedure operated on the assumption that "the change in friction factor is linearly proportional to the change in the hole diameter." It offered the advantage of allowing the analysis of HET data independent of the erosion delay. When there was no delay in erosion, the analyzed results were like the original method. Additionally, the modified procedure enabled the estimation of erosion rates and shear stresses in an HET based on only a portion of the data. For instance, in the case of hole blockage, the modified procedure allowed the continuation of the test and analysis of data after removing the blocked material from the hole [56].

Wahl et al. (2008), the United States Bureau of Reclamation USBR, USA

The Hole Erosion Test underwent significant refinement at the United States Bureau of Reclamation (USBR). This research program at the USBR led to notable enhancements in both the apparatus and data collection procedures initially proposed by Wan and Fell. Key improvements included [55]:

1. Measurement of flow rate using a custom 10° v-notch weir positioned at the downstream end of the setup.

2. Implementation of automated head measurements upstream and downstream of the soil specimen, as well as at the v-notch weir, utilizing pressure transducers and a computerized data acquisition system with recording intervals of 5 seconds throughout a test.

3. Introduction of a high-head HET setup capable of producing test heads of up to 7.68 psi.

4. Incremental doubling of the test head during an HET until progressive erosion was observed, starting at a low-test head, typically 0.07 psi.

The USBR also identified five major issues influencing HET interpretation:

1. identification of erosion regimes,

2. curve fitting procedures,

3. distinguishing between laminar and turbulent flow,

4. variation of friction factors,

5. and Determination of final hole diameter and length.

Marot et al. (2011), Université de Nantes and the United States Bureau of Reclamation (USBR)

The Université de Nantes, in collaboration with the USBR, developed an analysis method utilizing both the HET and JET. This method relies on fluid energy dissipation and the measurement of eroded mass, offering a distinctive erodibility classification for tested soils. In the HET, the energy dissipated by erosion, represented by frictional head loss, is correlated with the measured hydraulic gradient and flow rate [55]. The analytical approach involves applying an energy balance equation for the fluid between the upstream and downstream points, where hydraulic heads are measured at the sidewall of the flow chamber. This

equation considers minor head losses due to fluid entering (flow contraction) and exiting (flow expansion) the axial hole, assuming consistent average velocities in both measuring sections [57]. The assumption is made that the hydraulic head difference across the soil specimen is equivalent to the total energy head loss, which is the sum of friction and minor energy head losses. Through a series of HETs conducted on a non-erodible poly-acrylic model of the specimen with a predrilled 0.24 in. hole, an empirical constant was derived to isolate unknown friction head losses responsible for erosion. Remarkably, it was determined that, for this specific hole diameter, only approximately 25 percent of the measured hydraulic head difference across the soil specimen is attributed to wall friction [57].

Luthi, M. (2011), The University of British Columbia, Vancouver, Canada

A modification to the Hole Erosion Test (HET) was implemented by integrating a conventional static Pitot tube on the side of the test specimen, enhancing the analysis of energy-based data. Termed HET-P, this test introduces an additional measurement of the total energy load and velocity load at the point where water exits the preformed hole [47].

Consequently, it offers a simplified and more direct estimation of the axial hole diameter and corresponding erosion parameters without the need for assumptions regarding the hydraulic roughness of the axial hole, a requirement in the standard HET [49]. However, velocity measurements are influenced by flow conditions, necessitating a differentiation between laminar and turbulent flow.

Conducting tests on highly erodible and dispersive soils proved challenging due to the erosion process initiating upon wetting during sample placement and progressing rapidly once the test commenced. This rapid progression hindered the collection of sufficient high-quality data for representative and accurate analysis, diminishing confidence in the

interpreted results[47]. Furthermore, the Pitot-static tube's clogging by eroding particles was a prevalent issue in highly erodible and dispersive soils. Although the built-in backwash mechanism before each reading aimed to eliminate particles from the Pitot-static tube without disturbing the soil sample's bottom, its success was inconsistent. In instances where backwashing failed, the partially or totally clogged Pitot tube generated erroneous HET-P data [47].

Bonelli & Benahmed (2012), Irstea, Hydraulic Structures Research Group, France

This research group modified the device developed by Wan and Fell [49], changing the metrology, sample size, and type of hydraulic stress (controlled flow instead of pressure). The cylindrical cell, constructed from Perspex, is divided into three parts to allow visualization of the sample and detection of the erosion initiation. The inlet diameter measures approximately 3.15 in., while the outlet diameter is around 3.54 in. The central part is specifically designed to accommodate either reconstituted or intact soil samples.

Two pressure gauges are positioned at both ends of the cell, upstream and downstream, to measure inflow and outflow pressures, enabling a precise assessment of the hydraulic gradient applied to the soil sample. The upstream side of the device is linked to the incoming water and pressure regulator. The flow rate is regulated by an outflow vane and monitored by a flowmeter on the downstream side. Downstream of the cell, a turbidity meter is installed to analyze the outflow water and quantify the mass of soil transported during the flow. To homogenize the flow, a honeycomb structure is placed inside the cell at its upstream side [58].

Haghighi et al. (2013), Paris-East Créteil University, Paris, France

Haghighi et al. enhanced the traditional Hole Erosion Test (HET) by integrating a turbidimeter and a corresponding interpretation method based on analyzing the turbidity signal. The new method allows real-time estimation of instantaneous hole dimensions and eroded soil mass without relying on hydraulic assumptions. Results from various interpretation methods were compared, demonstrating comparability. The efficacy of the approach was tested on reference materials with different clay, silt, and sand mixtures, revealing the clay fraction's significant influence on critical shear stress and erosion coefficient. The study plans to extend the test to undisturbed, cored samples to diagnose erosion in existing earthworks [59].

Xie et al. (2018), Tongji University, Shanghai, China.

This article described the development of a HET apparatus designed for observing piping erosion and monitoring dynamic pressure conditions. The apparatus uses a transparent box to compact soil into a thin layer, allowing for the acquisition of dynamic hydraulic gradient information. A dismountable upper plate facilitates easy soil sample placement, and pressure sensors connected to capillary tubes measure dynamic pressure along the pre-cut hole. The pressure sensors are linked to a computer using RJ45 wire and controlled by the software which control water pressure sensors and record pressure readings. Flow regulation is achieved by adjusting the elevation of inflow and outflow constant-head tanks, with water temperature recorded to account for viscosity changes. The observable HET is conducted in a soil box with specific dimensions, featuring a pre-cut hole along the longitudinal axis to simulate a concentrated leak [60].

Bora et al. (2021), Institute of Technology Guwahati, Guwahati, India

The study introduced a new model based on the integration of Bernoulli's Energy equation and the work-energy principle using energy transformation to effectively depict the erosion processes within a hole erosion test where power acts as the driving force aiming to overcome limitations present in current methods. To validate the theoretical model, 24 HET experiments were conducted at various flow rates[61]. The proposed model, validated through experiments, can assess soil erodibility without requiring knowledge of the piezometric head. The experimental setup for the HET included three components: (a) an upstream water tank of 3.5 ft^3 PVC cylinder, (b) an eroding unit housing the specimen, and (c) an erosion collection chamber. The constant head between the two ends of the soil specimen was determined by the fixed height of the water tank. Adjustments to the water column height in the upstream tank were made to maintain the desired flow rates during experiments. The eroding unit had three sections, featuring screens, an air valve, and coarse aggregate for stabilization. The soil specimen had a pre-drilled hole to release radial confining stress, and the third part, the erosion collection chamber quantified eroded soil mass through vacuum filtering and oven-drying. This setup allowed direct monitoring of soil erosion without relying on flow assumptions [61].

Zaid et al. (2022), German Federal Waterways Engineering and Research Institute

Zaid et al. (2022) developed "The adapted hole erosion test" at the German Federal Waterways Engineering and Research Institute based on HET-P by Luthi in 2011 [47]. They introduced a novel approach to measure the hole diameter at different time steps during the HET using micro-computed X-ray tomography (μCT). Two HETs were conducted to investigate the relationship between friction factor and hole diameter, flow rate and time as well as the relation between hole diameter and flow rate [62].

METHODOLOGICAL APPROACH

Materials

The research used a commercially available BCSA cement. Some soil-cement samples were made with type IL portland cement for comparison purposes. The soil incorporated in the mixtures consisted of natural sand, play sand, and red art clay, at varying proportions as explained in the next section. Regular tap water was used in the mixtures. Food-grade citric acid was added in some cases. The mixtures were prepared using a benchtop mixer. Plastic freezer bags were used throughout each phase of the research to seal the soil during the curing period of the soil-cement cylinders.

Proportioning and Mixing

As mentioned before, all the existing guidance for proportioning soil-cement mixtures is based on using portland cement as the binder. Therefore, the substitution of BCSA cement required some investigation. From preliminary research presented in the 2021 MarTREC 6006 report [2], it was known that a mixture of 70 percent sand and 30 percent clay corresponded to an A-2-4 class according to the AASHTO classification system. The portland cement content by weight for such a mix was determined to be from 5 percent to 9 percent according to Table 1, based on this soil group classification. The 2021 report set the starting point for BCSA soil-cement mixtures by using this suggested portland cement content. In the same report, the optimum moisture content for a soil-only control group with the same proportion of sand and clay was 9.2 percent [2]. At the time, it was questioned whether the optimum moisture content for the soil only mixtures provided adequate water to reach proper cement hydration. Therefore, it was decided the first phase of the new research would focus on finding the optimum soil moisture to facilitate cement hydration. For this reason, a starting cement content of 6 percent by weight of soil was chosen as a continuation

of the past work, but after erosion testing, BCSA cement contents of 3 percent and 1 percent were also included. Two trial water contents were tested (7.5 percent and 10 percent), one below the optimum moisture content of the soil and one above the optimum soil moisture content. Initially, the same combination of 70 percent sand and 30 percent clay was used similar to the 2021 MarTREC study. Towards the end of this project, a few specimens with 85 percent sand and 15 percent clay were also tested, to compare how a weaker soil, that contained half the content of clay would perform when exposed to the piping phenomena simulated by the HET compared to the original mix.

Mixing and Compaction Procedures

Before mixing, the soil to be used was oven-dried, cooled to ambient temperature and properly stored so the moisture content was closely controlled. The soil mixture and water were combined one day before the cement was added. The desired proportions of dry sand and dry clay were placed in a bowl, then water was added to achieve the target moisture content. Once water was added to the bowl, the components were blended with the help of a benchtop mixer and then stored in a sealed plastic bag until the next day. The cement was then blended into the soil about 24 hours later using the mixer and then it was immediately compacted. For the mixtures that contained citric acid, the citric acid was added to the soil and water the day before compaction. The citric acid content by cement weight was fixed at 0.35 percent, which was determined through temperature testing, described in the testing section, to provide about 51 minutes between the addition of the cement and the setting time of the soil-cement material.

Proctor test procedures and equipment following the Standard Test Method for Laboratory Compaction Characteristics of Soil Using Standard Effort ASTM D698[63] were used to compact all cylinders. However, the mold used to compact the unconfined compressive

strength samples deviated from the mold described in the ASTMD698 standard to ensure the 2:1 height-to-diameter ratio required. The mold had a volume of 37.2 cubic inches and was 2.9 in diameter. To ensure that the sample was subjected to the same intended energy by the standard procedures, the number of blows per layer was adjusted and calculated to be 16 blows per layer; these layers were manually compacted with a standard 5.5 lb. rammer as described in the standard. On the other hand, the samples to be tested for erosion in the hole erosion apparatus were compacted following ASTMD698 [64] with no deviations. The standard, 4 in. diameter proctor mold was used, and layers were compacted using an automated proctor machine with a 5.5 lb. rammer that was mechanically operated as specified in section 6.2.2.1 of ASTM D698.

Sample Curing

The soil-cement cylinder curing period was assumed to initiate immediately after compaction and removal of the specimen from the compaction mold. Different curing conditions were implemented. In the early stages, cylinders were placed in a closed cooler for the desired curing time, but the cylinders were found to be losing their moisture content too quickly and drying out. To counteract this, a humidifier was set to 30 percent humidity level and placed inside the cooler with the cylinders. This method caused the cylinders to lose their shape and disintegrate. Thus, the third and final curing alternative that was studied was placing the compacted coil-cement cylinders in a sealed plastic freezer bag during the curing period in order to prevent rapid moisture loss and avoiding providing excessive humidity that led to deformation. The plastic bag alternative was the one that was observed to provide the best curing conditions for the cylinders, therefore it was used for all the tests that presented herein.

Effect of Continued Mixing on Performance

Initially, there was a question as to the optimal mixing time and the impact of mixing after a BCSA soil-cement mixture began to hydrate. For this reason, one of the first tests consisted of a mixture of 70 percent sand and 30 percent clay with 6 percent BCSA cement content at 10 percent MC and no retarder. This mixture was prepared identically to all the other mixtures but deviated from others in that it was not compacted immediately after blending; instead, it was mixed repeatedly for 5 minutes followed by 5 minutes of rest throughout the entire curing period of one hour. Given the short setting time of BCSA (as brief as 15 minutes), this intentional disturbance throughout and post-setting time aimed to assess its impact on strength. Therefore, one hour after the initial mixing, the sample was compacted and then tested for unconfined compressive strength. Under this regime, the sample exhibited extremely poor strength, and failed by abruptly essentially disintegrating with very little load applied, as shown in Figure 2. This empirical evidence underscored the critical importance of allowing sufficient working time with set retarders and compacting the soil-cement mixture prior to its setting time.

Figure 2. Sample compacted after initial setting time

Temperature Test to Determine Retarder Effect on Setting Time

The primary advantage of BCSA cement for soil-cement is its rapid setting time and strength gain. The time elapsed between mixing and placement of the soil-cement material in the soil-cement construction handbook is limited to about 60 minutes for portland cement, with travel time limited to 30 minutes. The setting time of BCSA can be as brief as 15 minutes after it is in contact with water, yet being consistent with the existing construction handbook, an extended and viable time frame for its on-site application is about 60 minutes. Consequently, food-grade citric acid which is a popular retarder for BCSA cement for concrete mixes, was employed as the retarding agent for the soil-cement blends. In this context, it became imperative to ascertain the extent of delay induced by the inclusion of citric acid within the soil-cement mixture. To determine the effectiveness of different dosages of citric acid with BCSA, the internal temperature of the soil-cement was monitored during the initial hardening

process of the cylinders. The standard soil mix with 70 percent sand and 30 percent clay was used with a BCSA content of 6 percent by weight, and a target moisture content of 10 percent. The percentage of citric acid in the mixture was varied to provide a range of expected setting times between 20 minutes and 2 hours. The citric acid doses that were tested were 0, 0.15, 0.35, 0.45, 0.50, and 0.70 percent by weight of cement. The test consisted of mixing and compacting the soil-cement specimens as described in the previous section. After the demolding of the sample, a digital thermometer with a probe was inserted into the center of the top face of the compacted cylinder and the initial temperature was recorded, immediately after, the cylinder was placed in a plastic bag that was kept closed for a few minutes until the next temperature reading was desired. The temperature readings were taken every 5 minutes and the thermometer was left in the sample until the value was relatively stabilized. Once the changes in temperature became larger every 5 minutes, it was known that the time to reach the cylinder´s maximum temperature could occur soon, therefore the temperature was tracked more frequently, at intervals as short as 30 seconds. Figure 3 shows the cylinder curing in the plastic bag while its temperature was being tracked. The test ended once the temperature was seen to decrease, as it was assumed the initial hydration peak was captured. The time elapsed between the addition of cement to the mix and the time of peak temperature was defined as a rough approximation of the setting time of the material. Figure 4 shows that citric acid affects the setting time of BCSA soil-cement mixtures linearly with increasing dosages, as is seen in concrete. A setting time of around 51 minutes post mixing is accomplished when using 0.35 percent citric acid by weight of BCSA cement.
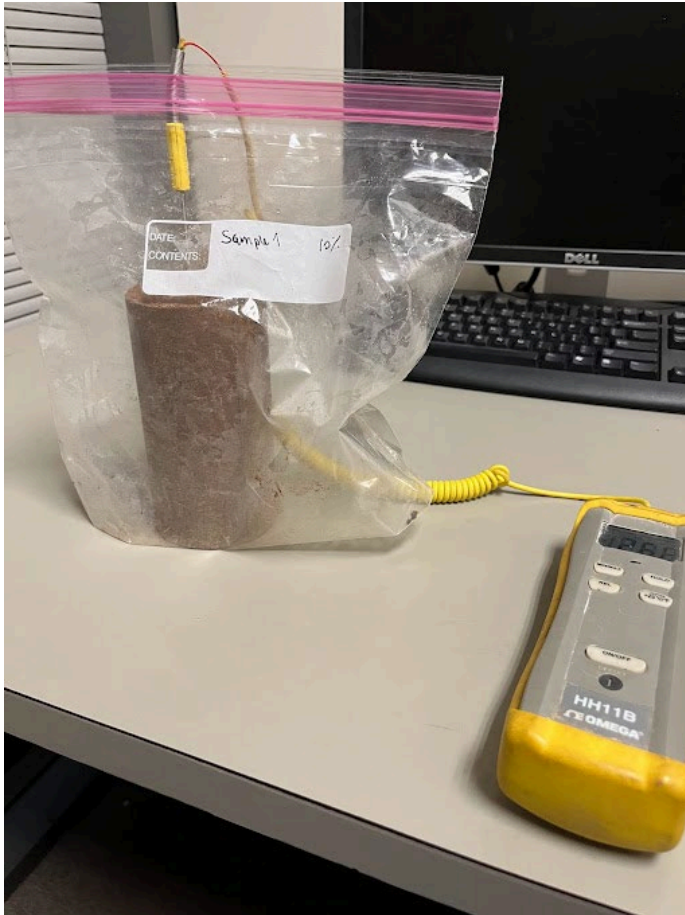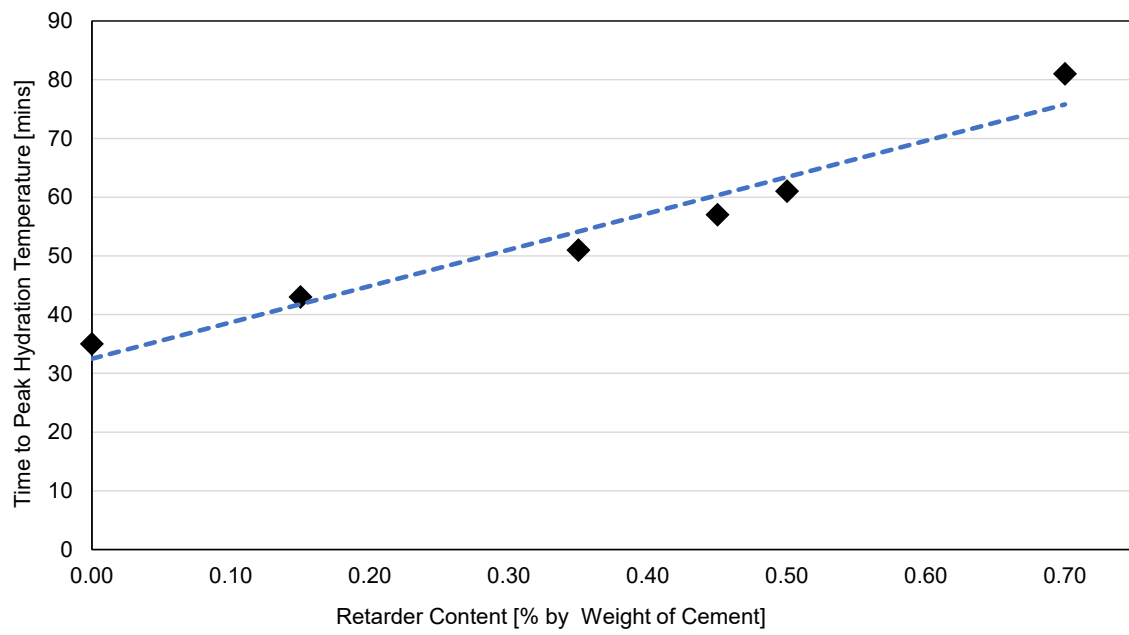
Figure 3. Retarder peak temperature setup

Figure 4. Retarder effect on setting time according to dosage.

Unconfined Compressive Strength Tests

Even though the soil-cement mixture had already been tested for strength in the previous phase of the project [2], it was decided that since the curing conditions had been modified, the uniaxial compressive strength tests should be performed again. At the end of the curing period of interest, the ultimate compressive strength of the material was determined by following the uniaxial unconfined compressive strength procedure described in the standard ASTM D2166 [65]. The testing was performed using a data acquisition system that was connected to a universal load cell with the load applied at a strain rate of 1 percent per minute.

A total of 46 cylinders of the mixture of 70 percent sand and 30 percent clay, later referred to as (70/30) soil mix, of various contents of BCSA cement and varying water contents and time were tested. Table 3 summarizes the number of cylinders tested per each mix and the varying moisture contents (MC) and ages tested. The optimum moisture content for the 70/30 soil, was reported as 9.2 percent water in past MarTREC 6006 report [2].

Of the 46 cylinders, a total of 30 corresponded to soil, with 6 percent BCSA content. Cylinders were tested at an MC drier than optimum and wetter than optimum MC of the 70/30 soil, therefore 7.5 percent and 10 percent MC were tested. Later in the studies, it was decided that for the same cement content a MC of 13 percent was tested as well, since the 7.5 percent MC cylinders seemed to be quite dry due to the hydration of the cement. A dosage of 0.35 percent retarder was used in the cylinders indicated in Table 3 to delay the setting time to about 50 minutes after mixing.

Table 3. Cylinders tested for 70/30 soil with various BCSA cement contents

70/30 Soil					
Group ID	Soil MC	% BCSA (by weight of soil)	Retarder (by weight of cement)	Curing Period	# Samples Tested
C7.5	7.50%	0%	No	1 hour	3
		0%	No	7 days	1
B6 7.5		6%	No	1 hour	2
		6%	No	7 days	2
B6R 7.5		6%	0.35%	1 hour	2
		6%	0.35%	7 days	3
C10	10%	0%	No	1 hour	2
		0%	No	7 days	3
B6 10		6%	No	1 hour	4
		6%	No	7 days	4
B6R 10		6%	0.35%	1 hour	6
		6%	0.35%	7 days	2
B3 10		3%	No	1 hour	2
B3R 10		3%	0.35%	1 hour	2
B1 10		1%	No	1 hour	3
B6 13	13%	6%	No	1 hour	2
		6%	No	7 days	3
Total					46

Modified UARK HET Development

The UARK HET system closely aligns with the original design by Wan & Fell [49]. However, a notable modification involves the water supply mechanism. In contrast to employing a tank that is elevated to enhance hydraulic load, a hose directly connects the water source to the system (Figure 5). Control over the flow rate and hydraulic load is achieved manually through a rotational gate valve, allowing adjustment by opening or closing the valve. This section discusses the initial setup, design, and modifications made to overcome different problems throughout the investigation, as well as a camera system that was developed and incorporated to improve the measurement of the hole diameter during the test.

The historical issue that persisted in the previously described HET setups was the turbulence in the downstream flow tank [49]. This turbulence can cause disturbances to the differential

pressure measurements and ultimately cause the results to be inaccurate. This issue was the main concern when designing a new and improved setup. The proposed solution was an extended up- and downstream flow tank to allow the flow to calm and stabilize before the pressure reading was taken. The flow tanks were proposed to be 24 in. long while keeping the same diameter as in previous setups.

The next issue that was described by other authors was the inability to test high strength soils as the pressure required to test such materials was not possible with an upstream tank on a pulley system on a wall (unless a 50 ft wall is readily available). Several ideas were discussed, and the first iteration was using a pump system with a large water tank attached such that the water could be recycled during the test.

The pump system was able to produce pressure up to around 20 psi (which equals about 50 ft of wall in terms of head pressure) and to pump enough water to maintain this pressure even at soils with high erodibility which would result in large, eroded diameters in the sample. The pump system, as shown in Figure 5, consisted of two pumps that fed into one pipe with a pressure port connected to a transducer to measure the pressure in the system before reaching the HET. The pumps could be run individually or at the same time to get a higher flow rate. A pump control valve was placed between the pipe and the pressure port so that the pressure in the system was controlled and able to be adjusted throughout the test. The outflow pipe from the pump was then connected to the upstream flow tank.
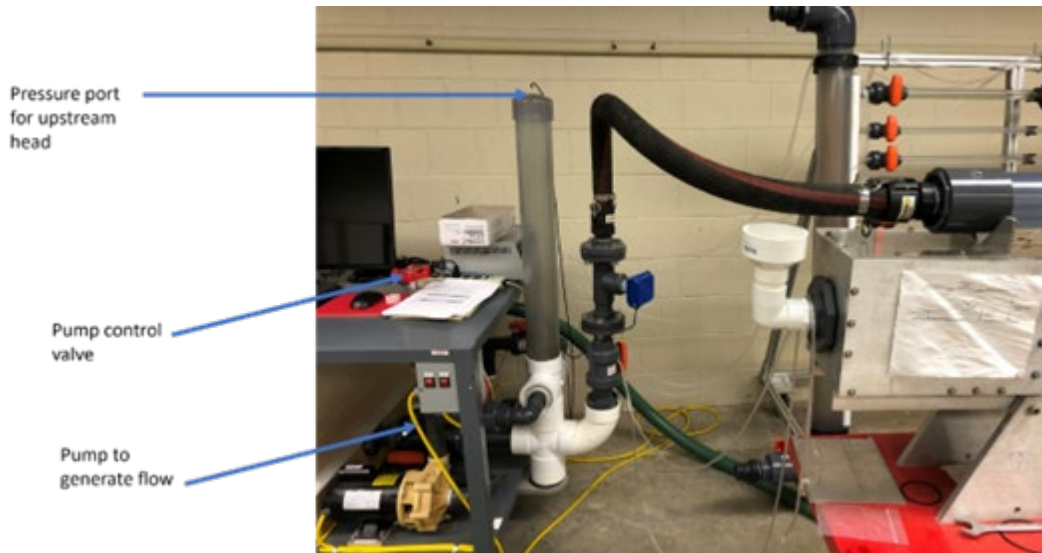
Figure 5.UARK HET iteration 1 – upstream pump system

This first iteration of the UARK HET was functioning well, and the sensors were reading correct values according to the pressure head and differential pressure calculations; however, there were a few issues with this setup. The main issue was the pressure from the pump was not able to stay constant and had a large amount of noise. As the test carried on, the pressure from the pump would fluctuate without changing the position of the gate valve that controls the inflow to the flow tank and sample. This seemed to be an issue with the performance of the pump rather than any issues in other places of the system as this issue was only experienced periodically and only if the system was run for an extended time at the same flow rate and pressure. This was an issue that could not be overlooked as constant pressure is vital when performing a HET. Many different options and valves were tested, and the conclusion was that the sporadic performance of the pump was not feasible to continue with the development of this setup.

Additionally, when using the pump and recirculating the water, the turbidity of the water became an issue when trying to incorporate a submersible camera system into the downstream flow tank to record the sample and the erosion of the sample during the test to

obtain a more accurate method of determining the soil's erosion characteristics. Reusing water in this test was particularly problematic when testing soils with higher clay contents as the clay particles stay suspended in the water. This was not a problem if the test was performed using only the water in the reservoir attached to the pump, but the amount of water used for this test exceeded the amount of water that the tank could hold. Several different filters placed at the reservoir were tested but none of the options were feasible.

The second iteration of the UARK HET needed to maintain a consistent flow rate and head pressure while providing clear enough water that a submersible camera could record the sample from the downstream flow tank. The solution to these issues was to connect the upstream flow tank directly to a hose that connects to the water supply line in the laboratory. This allowed for clear water to pass through the system and a consistent flow rate and pressure. A gate valve was added between the spout and the upstream flow tank. A photo of the second iteration of the system is presented in Figure 6.
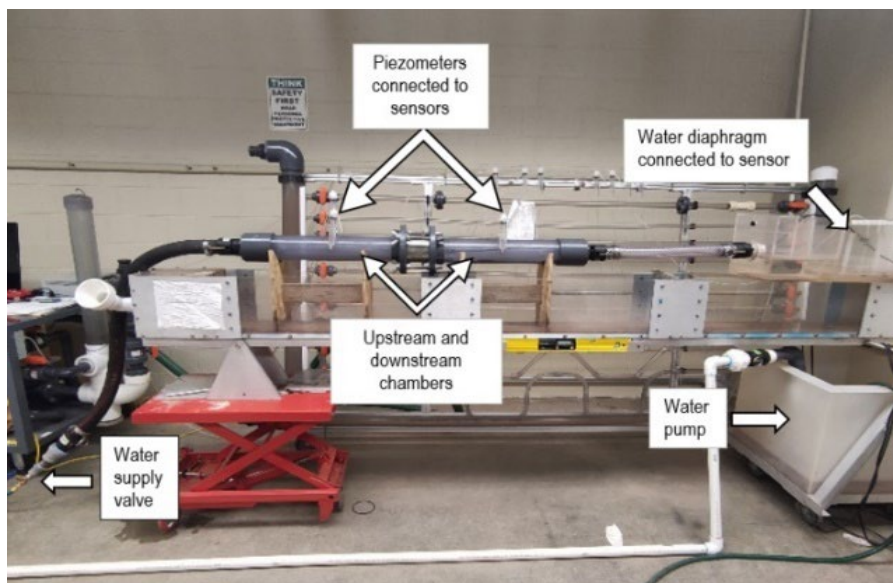
Figure 6.HET-UARK iteration 2 - setup and components

The downstream flow tank is identical to the upstream tank and both flow tanks are connected to the inflow and outflow conduits by polypropylene banjo cam lever couplings to allow for easy assembly and disassembly. The downstream flow tank is connected to another pipe leading the water to the downstream water collection basin with a constant pressure head. This downstream basin consists of a tank with two separate basins. The first basin is the collection basin for the water exiting the downstream flow tank. This basin has a constant pressure head to allow the pressure in the HET system to stay constant before the test has been initiated. Once the test has been initiated, the water overflows into the second basin. This basin consists of a v-notch weir to determine the flow rate during the test. In the basin, a submersible diaphragm connected to a pressure sensor was placed such that the water level in the v-notch weir could be digitally recorded during the test. The sample is a standard proctor mold which is fastened by four all-thread bolts and nuts and the soil is placed between the two flow tanks and secured by tightening these bolts such that no leak is present. Any leak would be serious as the pressure differential would be incorrect during the test.

The upstream and downstream chambers each had a length of 24 in., an inner diameter of 4 in., and an outer diameter of 4.25 in. to properly fit the standard Proctor mold containing the sample. To ensure zero slope across the HET chambers, an adjustable platform was used under one side of the system and a level was used while setting the initial height.

To monitor and record the pressure difference between the upstream and downstream chambers, an NPX MPX5700 sensor, along with a 1608FS USB acquisition card connected to piezometers, was utilized. Simultaneously, the water diaphragm was linked to an NPX MPX5010 sensor, paired with a 1408FS USB acquisition card, which was employed to measure and record the flow rate. Real-time interpretation of the data during the test execution was facilitated by a program developed in Agilent Vee, a language for data

acquisition and control. This setup allowed continuous monitoring of variations in both differential pressure and flow rate. Data were stored at 10-second intervals by the acquisition cards, while the program interface provided observations at 1-second intervals. The initiation of the erosion process was inferred when the differential pressure started to decrease during the test, while the flow rate remained constant, as an indicator that the hole through the sample increased in diameter.

After testing with the second UARK HET setup, the results were improved compared with the original setup, as were the variations in the pressure differential. However, it was difficult to achieve repeatability of the differential pressure increases in each test until the onset of erosion was reached, due to the high degree of sensitivity in the valve used, which also led to larger jumps in the flow rate values. Therefore, it was decided to use a new higher-resolution valve that would allow a more gradual flow rate step. Figure 7 shows the new connection between the valve and the upstream chamber for the final setup, while Figure 8 shows a schematic diagram of the entire setup.

Figure 7.Hose-valve-upstream chamber with connection for final setup
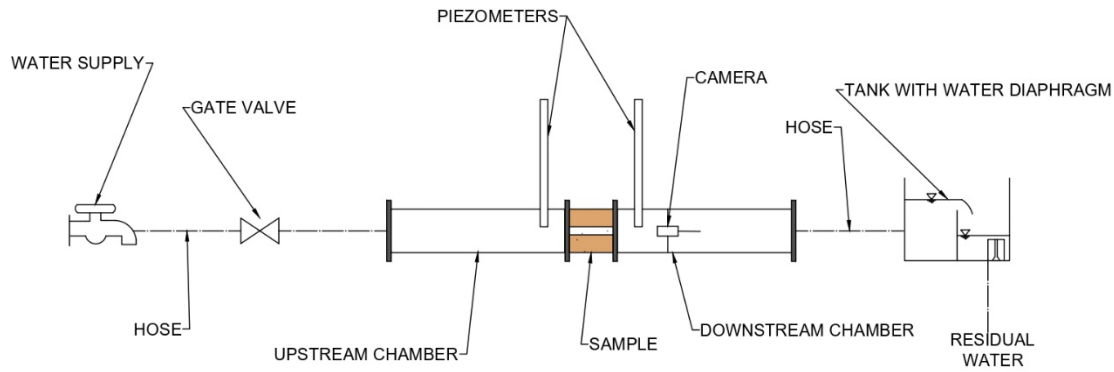
Figure 8.Schematic diagram of final HET-UARK

Calibration of Sensors

The flow sensor calibration was conducted using two calibration samples with PVC cylinders of varying diameters surrounded by plaster of paris. The first one consisted of a PVC cylinder of 0.6 in. diameter, referred to as "PVC Small" and the second one consisted of a PVC cylinder of 1 in. diameter referred to as "PVC Big". Each of these cylinders was affixed in the HET, the system was initiated, and the computer program for recording voltage and flow readings was started. Simultaneously, manual water collection was performed at the system's discharge area, with timing intervals adjusted as per the flow rate. For lower flow rates, a one-minute collection was executed, while higher flows necessitated a larger volume bucket (flows exceeding 5.3 gal/min reached the bucket's capacity in about 20 seconds). These manual readings were then plotted alongside the corresponding voltage values from the flow sensor data collected in the computer. The relationship between the manually measured flow and the voltage output from the sensors is presented in Figure 9. The polynomial trend equation in the plot was used to convert measured voltages to flow rates during the test. As shown Figure 9, despite the variance in diameter, the data showed that the flow through the system was conserved, and the data followed a trend of an order 4 polynomial equation. Therefore, the flow sensor was calibrated with such equation.
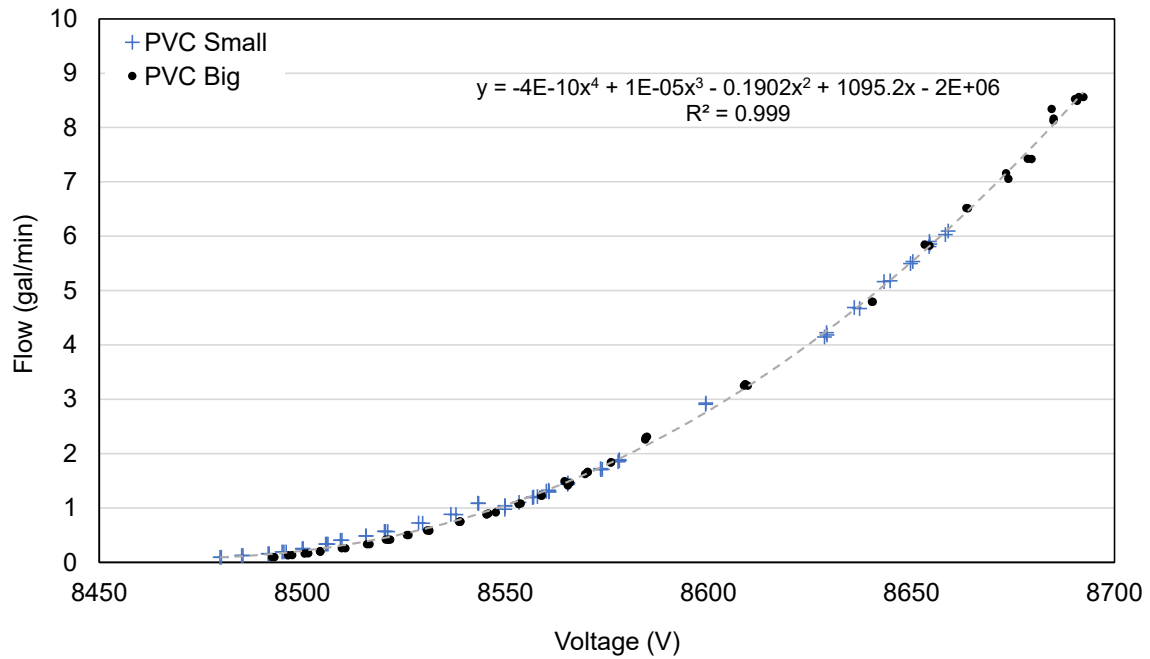
Figure 9. System calibration for calibration PVC plaster of paris samples

Design and Calibration of Camera System

One of the major criticisms with previous HET methodology lies in the assumptions of the empirical equations with the increase of the hole size throughout the test. With the test setups in the literature, the diameter of the hole is only known at the beginning of the test and at the very end. There is no measurement of the diameter of the hole at any point during the test. This means the estimation of the erosion rate and shear stress introduces error into the method and only one pressure head can be tested at a time as opposed to an erosion function such as what is measured in the EFA. Additionally, if the sample starts to erode before the system detects an increase in flowrate, the initial hole diameter will be incorrect.

This investigation introduces the use of a submersible camera inserted in the downstream flow-tank to accurately measure the hole diameter at each interval of pressure along with a reference marker at the downstream side of the sample printed scale, as shown in Figure 10. The addition of the reference scale makes it possible to get an accurate measurement of the

eroded hole size regardless of the placement of the camera and focal length. At the completion of the test, the images were processed using a Segment Anything Model with Python to determine the exact diameter of the hole. In theory, the tests performed with the camera setup should show a slightly lower erosion rate and erosion index as the change in the eroded specimen will be lower than with a measurement before and after the test.

Figure 10.Calibration marker on the downstream hole of an eroded sample.

The camera used for this for this method was a NTS300 Pro Auto-Focus Inspection Camera which includes an illuminated lens and 9.8 feet of probe length which can be seen in Figure 11a) For this method to work consistently, a holder for the camera itself needed to be developed such that the lens is located at the center of the flow tank and the angle of the image taken is as close to level with the sample as possible. Several different designs were developed and tested but one design worked better than the others. The design involved 3-D printing a cylinder that surrounded the lens centering it in the flow tank. The holder and support can be seen in Figure 11b).

Figure 11.(a) Viewing screen and operating controller, (b) Camera shown with holder and 3D printed support

Camera System Verification

A verification study was undertaken with the camera integrated into the system to ensure it did not impede the flow or compromise the accuracy of the tests conducted on the soil-cement cylinders. The camera was placed at a position of 2, 4 and 6 in. away from the hole downstream of the sample. The system was started and similarly to the calibration procedures, water was manually collected in time intervals to find the flow and compare it to the voltage recorded by the sensor. The data collected at the different camera locations was then compared to the trend of the original calibration of the apparatus when no camera was incorporated in the system. Therefore, since the data collected from the test that included the camera at different distances from the sample aligned well with the data collected when the camera was not present, it was concluded that the camera in the system caused no disruptions with the water flow (Figure 12 and Figure 13).. Figure 15 includes the data collected without

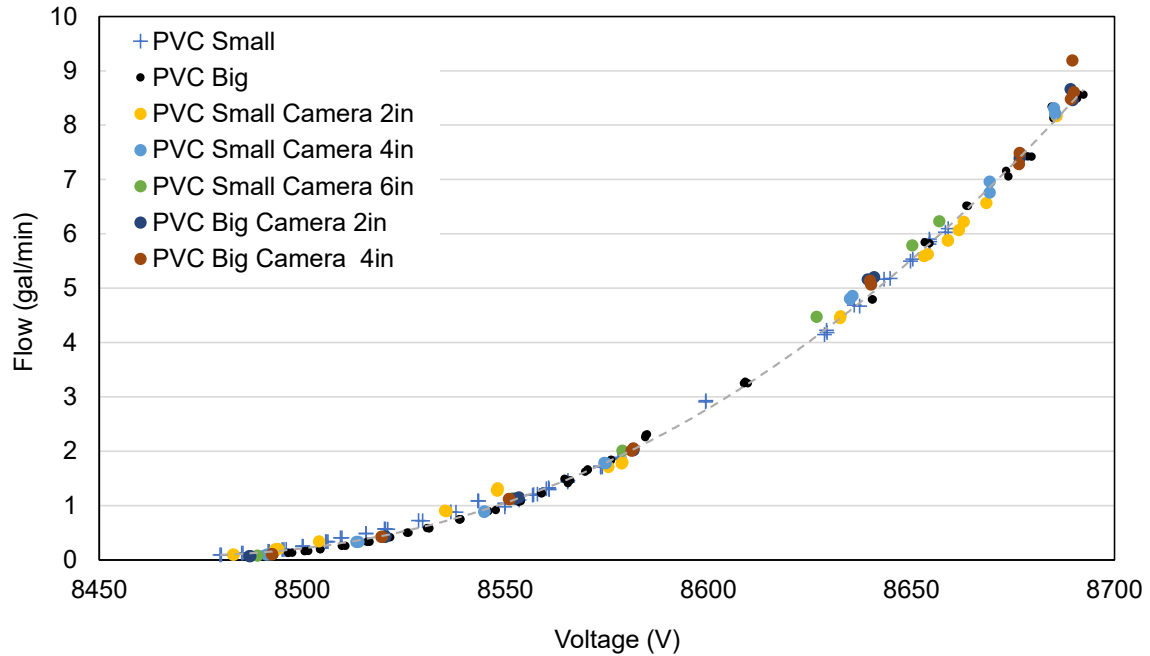the camera, and with the camera placed at varying distances from the downstream sample face.

Figure 12. Comparison of flow rate versus voltage with no camera and with the camera placed at different distances from the downstream sample face

The data followed a similar trendline, as shown in Figure 13. The incorporation of the camera into the system at different distances from the downstream hole showed a negligible effect on the flow rate. For visibility purposes and to prevent the camera from affecting the recirculation area caused when the flow exits at high velocity from the small sample hole it was decided to place the camera at distance of 4 in. or more from the downstream face of the sample into the UARK HET system.

The chart shows two polynomial trendlines with the following equations:

$$y = -4\text{E-}10x^4 + 1\text{E-}05x^3 - 0.1902x^2 + 1095.2x - 2\text{E+}06$$
$$R^2 = 0.999$$

$$y = 4\text{E-}10x^4 - 1\text{E-}05x^3 + 0.1672x^2 - 946.97x + 2\text{E+}06$$
$$R^2 = 0.998$$

Legend:
- Poly. (PVC Data No Camera)
- Poly. (Total Data Camera & No Camera)

Axes: Flow (gal/min) vs Voltage (V)
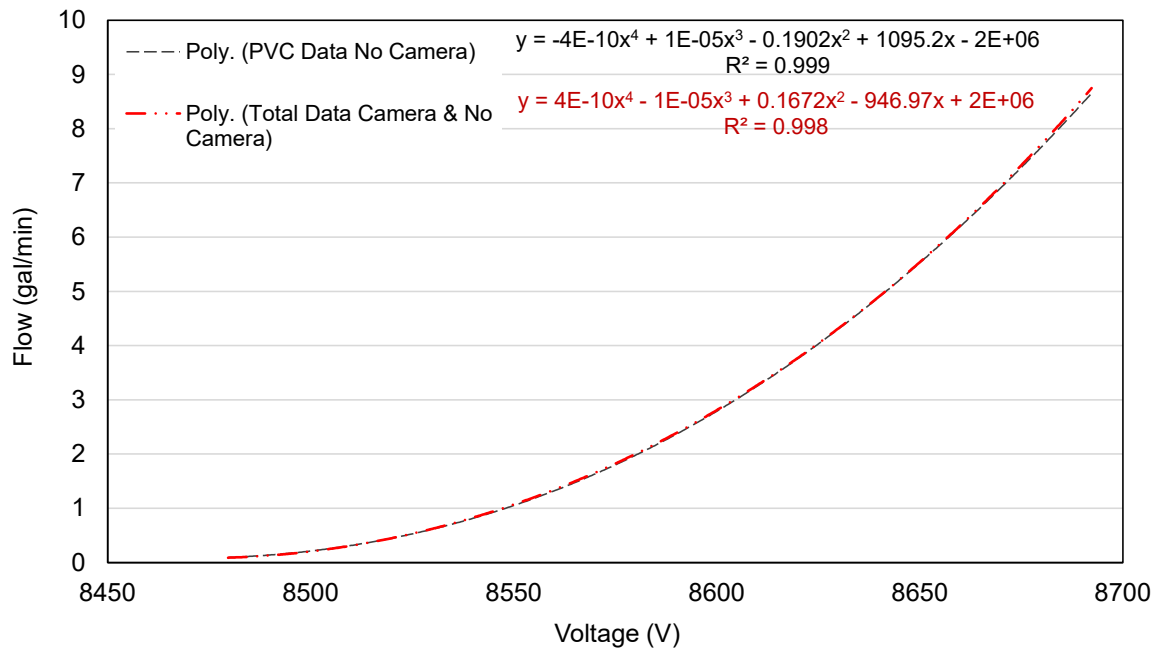
Figure 13.Comparison of data trendlines with and without the camera system integrated

Application of a Segment Anything Model

To process the data collected with the camera, a Segment Anything Model (SAM) was used

to analyze the images of the holes during the HET test. The model was integrated into a

Python code, where the image was initially loaded and the model was told, using Cartesian

coordinates, where the main hole was located. The model then provided three images where

the original image was segmented into different masks, and the image with the highest degree

of accuracy in the hole was chosen. Then, the model was given the coordinates of a circle and

square with known dimensions as a reference, to finally obtain the relationship between the

area of the hole and the geometric figures. Figure 14a shows a photo of a sample at the start

of a test and Figure 14b shows the same photo during the SAM segmentation process using
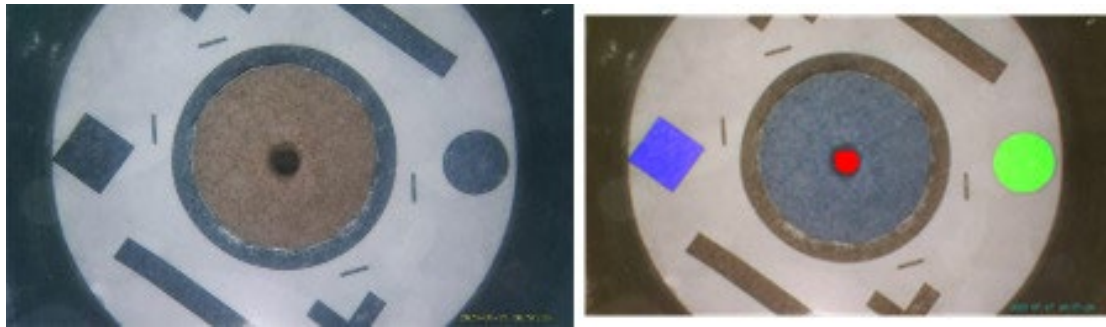
the calibration sheet.

Figure 14.(a) Sample at start of test with calibration sheet in place, and (b) segmentation of hole and reference circle and square on the calibration sheet during image processing

HET Procedures and Processing

Procedure During Test of Soil-Cement

The first step involved preparing the soil-cement sample and compacting it in the 4 in. mold. A portion of the excess compacted soil-cement sample was collected to determine the initial moisture content, then the compacted sample was placed in a plastic bag inside an insulated container until the desired curing time was reached. Before each test, the hole erosion apparatus was cleaned to ensure no residual soil was present in the pipes before a new test. The position of the submerged camera was adjusted to the proper location in the downstream flow pipe at an appropriate distance from the cylinder. Special attention was required for the O-rings that are placed between the upstream tank and the proctor mold and between the proctor mold and the downstream tank. These needed to be cleaned to avoid leaks during the test and any groves or surfaces in the cylindrical mold and fittings also needed to be cleaned. A layer of vacuum grease was applied to both sides of the rings and placed in the flanges to provide additional leak protection. After this, the calibration sheet was placed in the downstream tank flange. When that step was completed, the piezometers were connected to the upstream and downstream flow tanks. To make sure the flow sensor was properly calibrated, the diaphragm was adjusted to the proper level, and the water in the tank level was adjusted to be as close to the bottom of the v-notch weir as possible.

About 10 minutes before the time targeted for testing, the cylinder was removed from the sealed plastic bag, and a 0.236 in. (5/16 in. drill bit) diameter hole was drilled along the center of the soil sample to simulate piping. A frame and plate were used to ensure the hole was drilled in the center and perfectly vertical each time. Subsequently, the initial hole diameter was manually measured and recorded using a Vernier caliper. After the soil-cement specimen hole was drilled and the entire system was prepared for the start of the test, the soil-cement cylinder was then quickly placed into the hole erosion apparatus to ensure that the start of the test was at the desired elapsed time since the compaction. Once the mold was placed in the system, it was secured with four all-thread rods and bolts. Next, both upstream and downstream chambers are filled with water slowly and evenly, seeking not to generate disturbance that could change the initial diameter of the hole in the sample. Both flow chambers were filled simultaneously. A hose was used for the downstream tank, while the upstream side was filled by opening the gate valve slightly. When the two sides were full and the downstream tank was at the required water level, camera visibility was verified, and the test was started by starting the HET program in the computer to initiate the data recording.

With the program running, the data was monitored in real-time to determine if erosion was occurring. If the initial pressure differential was not sufficient to induce erosion (presented by a constant drop in differential pressure without an increase in flow rate), then the gate valve was opened slowly to increase the differential pressure in the system, using increments of 0.03, 0.07, 0.14, 0.21, or 0.28 psi., depending on the type of soil that was being tested. Low increments were used for soils that were more susceptible to erosion such as the control cylinders that had no cement, and higher increments were used for stronger (i.e., less erodible) soils containing cement. After each increment in flow, the system was left unchanged until the flow was stable, once the flow was stable, the tester determined if erosion was happening or if a higher increment of flow was necessary. Once the pressure

drop was observed, indicating erosion had started, the flow valve was gradually opened to try to maintain a constant pressure differential that initiated the erosion process. After each increase in the pressure differential, a photograph was taken using the camera to capture any increase in the diameter of the hole.

Once the maximum flow rate allowed by the system was reached or the soil was eroded sufficiently, the test was considered to have reached the end and the flow of water through the system was stopped. The mold with the sample was removed from the HET system, and using a Vernier caliper, the final diameter and the final length of the soil sample were manually measured.

Data processing and visualization

Once the data from the initial moisture content was gathered, it was copied into a Microsoft Excel template that was created to automate and facilitate calculations. The moisture content is used to compute the dry density which is used as a reference throughout the remaining calculations. The differential pressure and flow rate data from the file generated by the program in Agilent Vee in the "Raw Data" tab was then pasted into the spreadsheet. Figure 15 provides an example plot of the pressure differential and flow rate data collected for a test. It can be observed that the differential pressure for the 0.14 and 0.21 psi increments follows a mostly flat line, while the flow rate tends to increase slightly through time, which indicates that erosion is occuring.
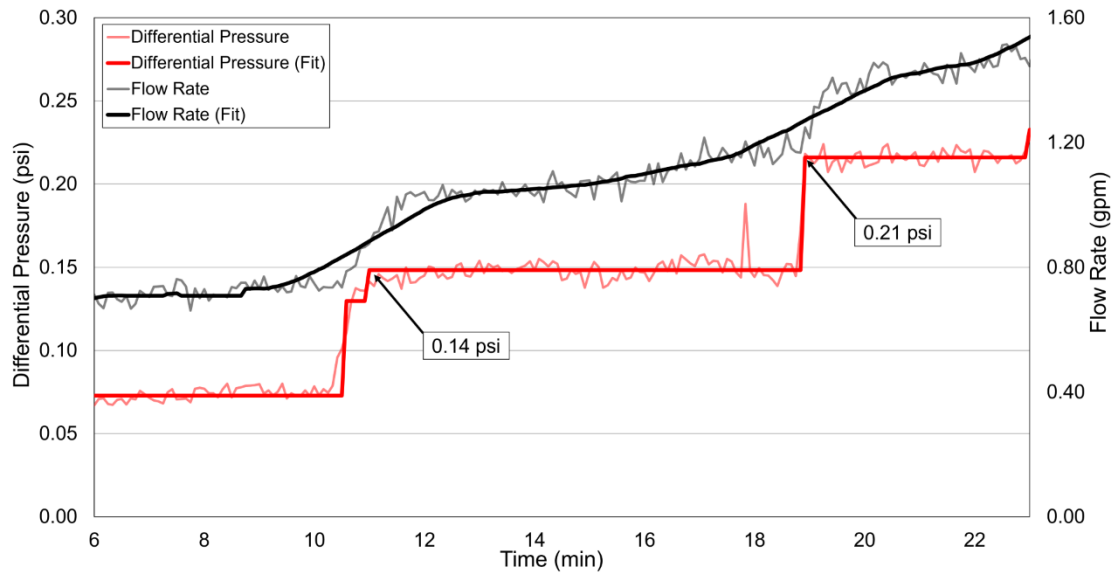
Figure 15. Example of differential pressure and flow rate data collected for this investigation

The water temperature (needed for kinematic viscosity), initial diameter, final diameter, water density, and length of the sample at the end of the test were entered into the datasheet called "Data Analysis" in the template. It was necessary to verify that the initial diameter in the tests was not affected by filling the upstream and downstream tanks, so using the SAM model program, each of the images taken at the beginning of the HET was introduced. The variation of the hole diameter, erosion rate, and shear stress throughout the test was computed by introducing previous data and flow rate and differential pressure values from the part of the data after erosion started. It was assumed that the length of the sample, which is reduced due to water removing particles in both end faces of the cylindrical sample, varied linearly over time. A second-degree trendline was used to approximate the change in diameter over time, as suggested by Wahl [20] and shown in Figure 16. Figure 17 shows an example of the determined erosion rate and shear stress developed using empirical equations from Wan and Fell [14].
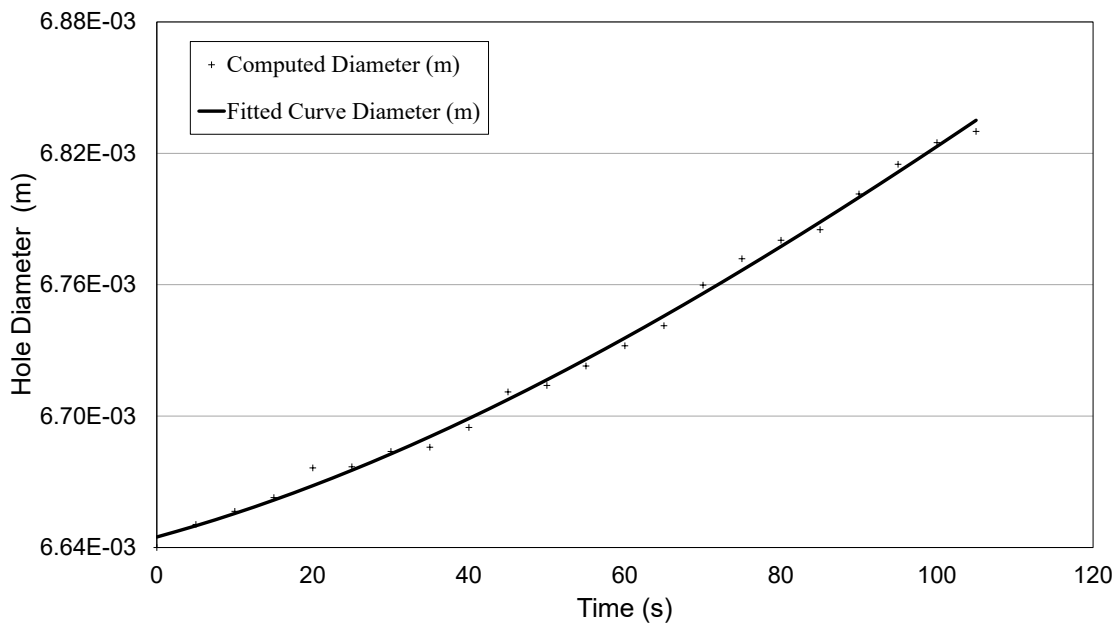
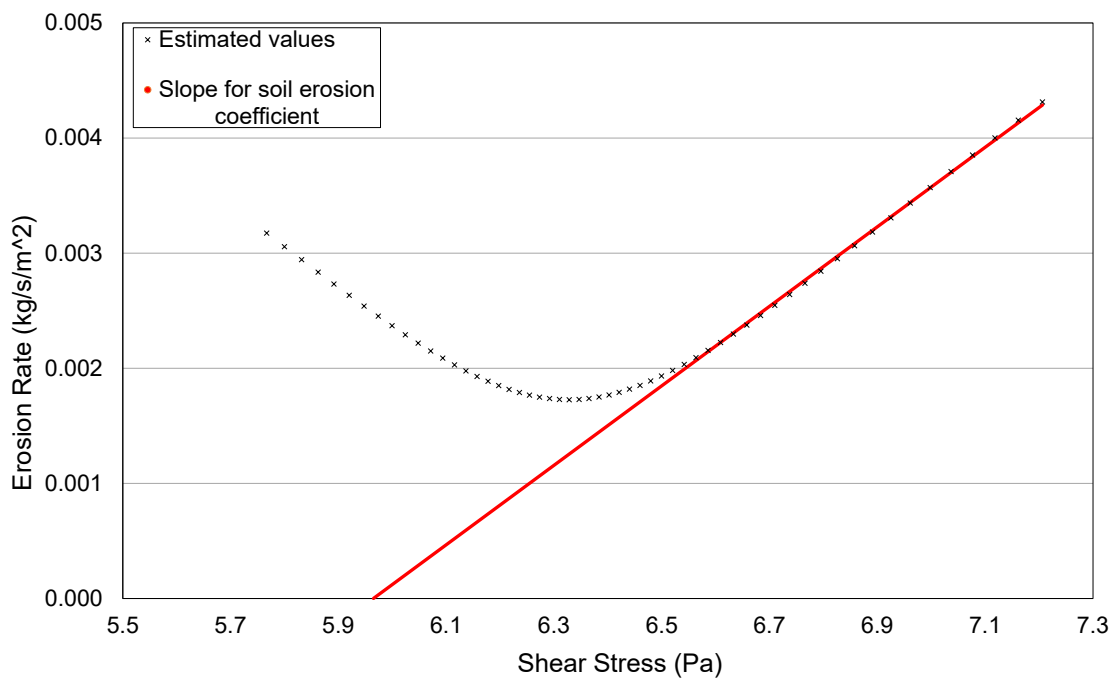*Figure 16. Example plot of the progression of hole diameter through time for the HET*

Figure 17. Example of the erosion rate versus shear stress plot throughout the test

Camera System Accuracy Verification

Table 4 presents the results for the comparison of the initial diameter, D_i, and final diameter, D_f used to verify the accuracy of the camera system. Hole diameters measured using Vernier calipers before and after the test and measured using the SAM during the test are shown for six soil-cement samples with cement content varying from 1 to 3 percent.

Table 4. Vernier caliper and SAM hole diameters comparison

Test	D_i Vernier (mm)	D_f Vernier (mm)	D_i Camera (mm)	D_f Camera (mm)	Error D_i (%)	Error D_f (%)
1	5.56	8.03	5.54	6.95	0.27	13.40
2	6.93	10.22	6.41	9.53	7.57	6.78
3	5.56	6.76	5.48	6.33	1.47	6.30
4	6.67	6.79	6.08	6.15	8.78	9.35

It was observed that for most of the tests, the difference between measurements with the vernier calipers and the camera presented less than 10 percent margin of error. Larger margins of error for the final diameters may be caused by the discrepancy in pictures that were taken at times of maximum flow, since at the end of the test, despite closing the tap immediately, part of the remaining flow continues to generate stresses along the sample hole. This is an important deficiency in classical HET interpretation because the caliper measurement at the end of the test may include some erosion that is not captured in the recorded flow data. These measurements can also be very subjective and user dependent.

In addition, the final diameter becomes much more irregular than the initial diameter, which could make it harder to evaluate using the calipers. The SAM algorithm identifies the outline of the hole and accounts for any irregular shape, and it then calculates an equivalent diameter based on the area of the hole captured. Overall, the camera system appears to provide a reliable and accurate method for obtaining hole diameters and it overcomes many of the

issues associated with measuring them by hand. Note this comparison does not consider the relationship between the actual diameter and camera-measured diameter during the progressive erosion, since it is not possible to use the caliper while water is running through the sample.

RESULTS

Unconfined Compressive Strength Results

Figure 18 shows the average compressive strength of the specimens with 6 percent BCSA cement content with varied moisture content (MC) at different curing ages. The curing ages tested were 1 hour and 7 days. The 1-hour age was selected because this is a very early stage of strength development for conventional portland cement, however, BCSA cement with no retarder starts setting as soon as 15 minutes, and for BCSA soil-cement cylinders that contained retarder, the period of interest (1h) was briefly past their setting time of 50 minutes. Figure 18, also includes 9 cylinders corresponding to the control group (labeled C), referring to the cylinder with no cement content. It is observed that the highest strength for all cylinders with 6 percent BCSA cement content was achieved at 10 percent MC with no retarder added. However, all the cylinders containing BCSA cement were significantly stronger than the soil only samples. The addition of citric acid reduced the 1-hour and 7-day strengths for every case, but it provided more working time for sample preparation which may be important for field operations and placement.
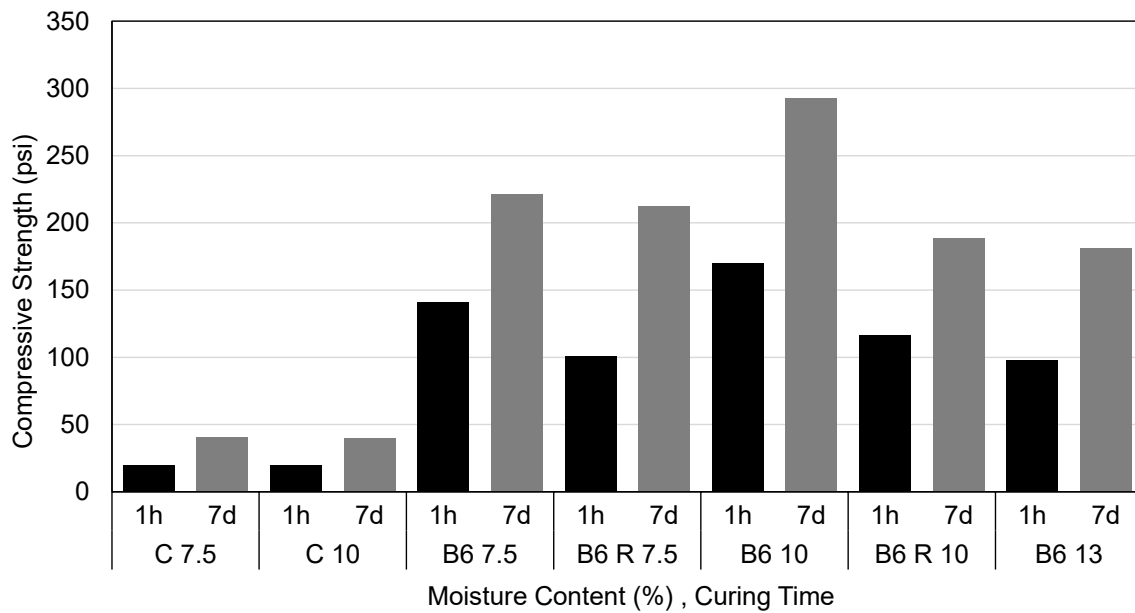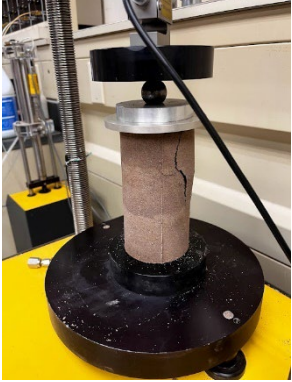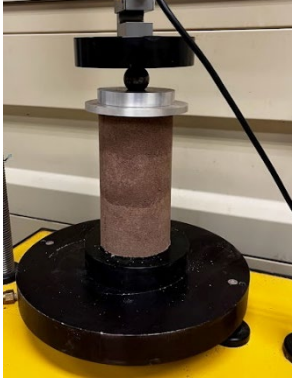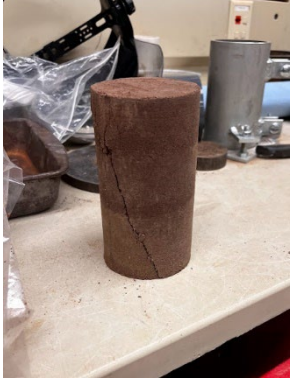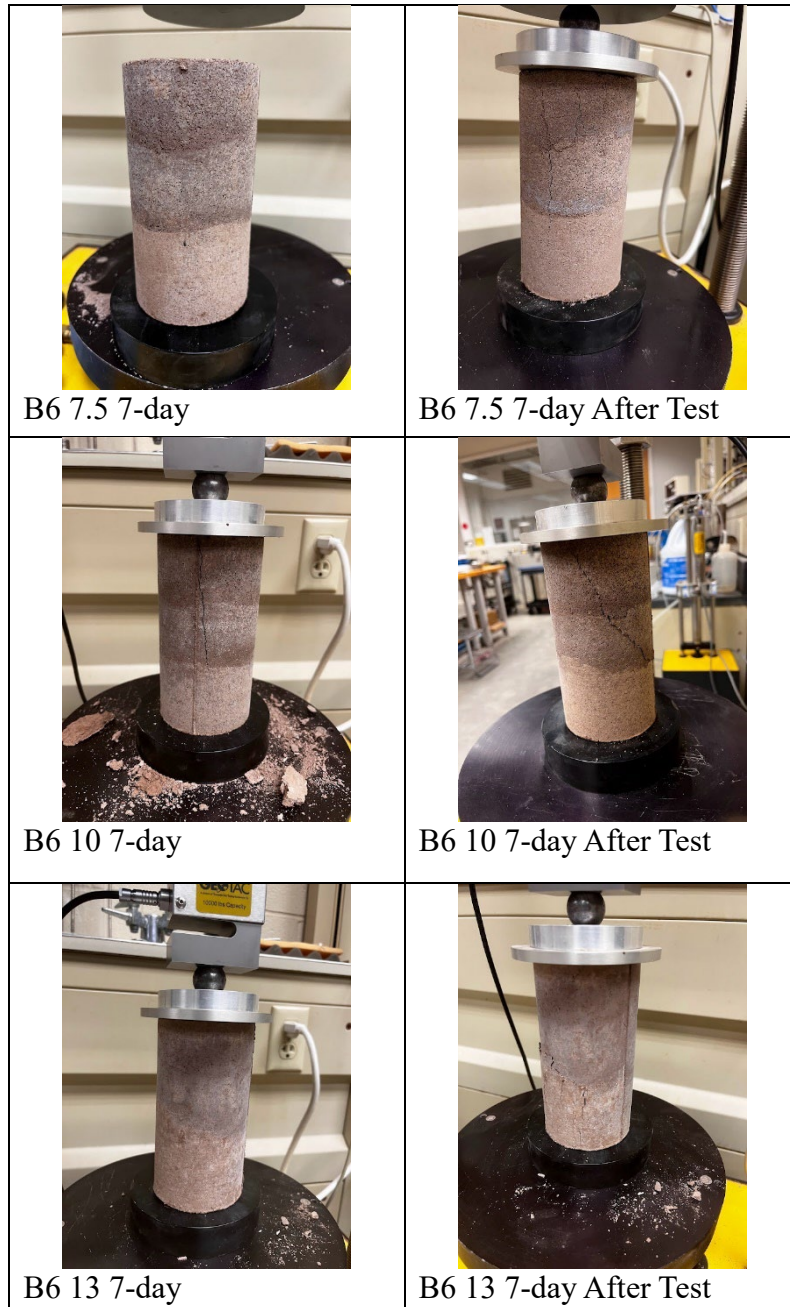
Figure 18.Average compressive strength of 70/30 soil per curing period and moisture content. Control sample with no cement (C) and samples with 6 percent BCSA cement content by weight are shown.

As shown in Figure 18, the 70/30 Soil cement samples with 6 percent BCSA cement prepared at 7.5 percent MC (dry of optimum) reported an average compressive strength of 140 psi after 1 hour of curing and 225 psi after 7 days of curing. Table 4 includes pictures of the samples with 7.5, 10, and 13 percent MC tested at curing times of 1 hour and 7 days. Cylinders that were 7 days old at the time of testing were significantly drier. At earlier ages, the 10 and 13 percent MC samples were more moist looking compared to 7.5 percent MC. Samples at 7.5 percent MC showed the lightest brown color for both ages and the failure of these cylinders was more irregular. Such discrepancies are attributed to an insufficient moisture content that adversely affected the hydration process of the cement and contributed to a non-uniform microstructure throughout the cylinder, therefore, the strength of the cylinders was unpredictable. Furthermore, the dryness of the samples made the demolding process challenging which could have led to damage of the cylinders.

Table 5. Samples with 6 percent BCSA by weight of dry soil at MC of 7.5, 10, and 13 percent for curing times of 1 hour and 7 days.

B6 7.5 1h	B6 7.5 1h After Test
B6 10 1h	B6 10 1h After Test
B6 13 1h	B6 13 1h After Test

B6 7.5 7-day	B6 7.5 7-day After Test
B6 10 7-day	B6 10 7-day After Test
B6 13 7-day	B6 13 7-day After Test

Better results were observed for mixtures that were wet of optimum MC. The highest average compressive strength was 170 psi for 1 hour of curing and 295 psi for 7 days of curing, both for MC of 10 percent. Samples at 13 percent MC reported consistent values of strengths, with an average of 100 psi after 1 hour of curing and 180 psi after 7 days of curing. However, their moisture content reflected by the darker color compared to the cylinders of lower MC, lowered their compressive strength.

The addition of 0.35 percent by cement weight of citric acid in the 6 percent BCSA soil-cement mixtures seems to decrease the strength even at later ages. Lower strengths were reported in the cylinders that were tested after 1 hour of curing but also in those tested after 7 days of curing. No retarder was added to the 13 percent MC. Strengths for retarded mixtures were 100 psi for 7.5 percent MC after 1 hour of curing, 225 psi for 7.5 percent MC after 7 days of curing, 120 psi for 10 percent MC after 1 hour of curing, and 190 psi after 7 days of curing. For the same 70/30 soil mix, 4 samples with BCSA cement contents of 3 percent and 3 samples of BCSA cement contents of 1 percent, with and without the addition of retarder were tested. For the samples containing 3 percent BCSA cement, the average compressive strength was 85 psi after 1 hour of curing and 85 psi with the addition of 0.35 percent retarder and all properties held the same. Therefore, it is observed that retarders could cause less impact on the strength when the cement content is lowered even when the retarder dosage is maintained.

Figure 19 shows the average compressive strength for the 3 percentages of BCSA content tested (6, 3, and 1 percent), as well as the control group. As the cement content increased, the compressive strength increased when other properties were held constant. The samples with 3 and 6 percent BCSA cement were very strong and exhibited zero erodibility in the HET even under the maximum flow possible. Erosion was first able to be detected in the HET for the mixtures with 70/30 soil and 1 percent BCSA. Thus, it was decided that conventional portland cement was going to be tested at this percentage, to compare the compressive strength of the samples made with BCSA cement versus portland cement. Figure 20 shows that a 1 percent BCSA soil-cement was 25 percent stronger than 1 percent portland cement at 1 hour after compaction.
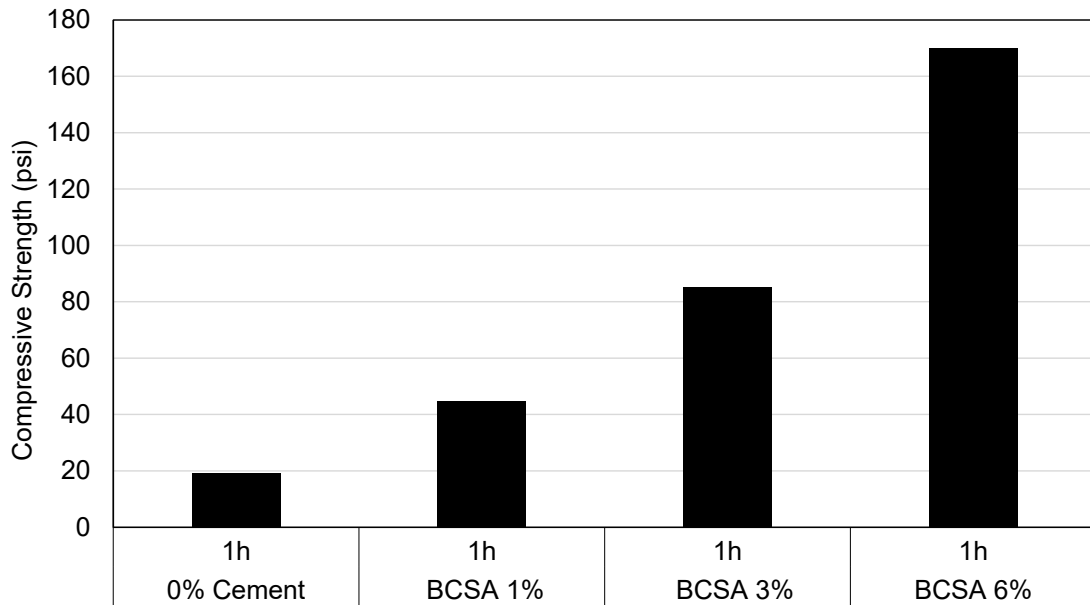
Figure 19. Average compressive strength of 70/30 soil at 1 hour curing period and 10 percent moisture content for increasing BCSA cement contents.
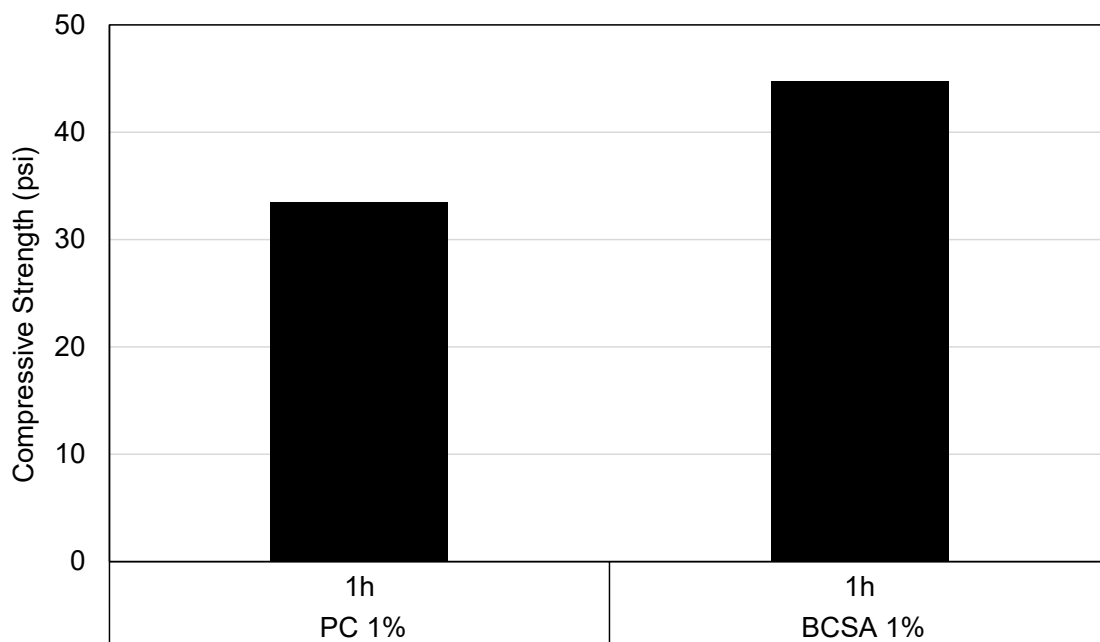

Figure 20. Average compressive strength of 70/30 Soil at 1-hour curing period and 10 percent moisture content for 1 percent BCSA versus 1 percent portland cement

HET Results

Tests were initially planned to compare the degree of improvement in the erodibility of soil-cement mixtures as the percentage of cement increased. Figure 21 presents the results for the average erosion rate index for BCSA cement and portland cement at 1 percent cement content with variations in time of curing and moisture content. The 10 percent MC samples were tested first since they had the highest strength based on the UCS testing. Afterward, the tests were performed with a 12 percent MC to evaluate the effects of increased moisture. The results for the erodibility performance after 1 hour of curing shown in Figure 21 present an opposite trend to the one obtained in the strength tests. Samples with 10 percent MC made of BCSA (which had higher strengths than the portland samples) showed a lower erosion index compared to portland. The graph shows that increasing the MC to 12 percent improved the erosion resistance of the soil-cement samples at all ages. Therefore, it was suspected that despite the hardening of the cement, the loss of water in the bonds between clay particles during this early stage resulted in a higher erodibility. It was suspected that a slight increase in MC could benefit the cohesion of the particles and increase their erosion resistance. Similar to what Burris [62] states, it could be concluded that drier soils (like concrete with lower water content) tend to present a higher erodibility due to microcracking. This could be compounded by the lack of cohesive forces provided by the soil moisture since some of that moisture is consumed in the cement reaction. The soil-cement could also be fractured while drilling the hole and could lead to increased erosion for the drier BCSA specimens as there would not be additional available water to continue the hydration process.

The plot also shows that more curing time corresponds to better performance against erosion, given the progressive hardening by the cement. When comparing the performance of BCSA and portland cement with under 12 hours of curing at 1 percent cement content and 12

percent MC, the results in Figure 21 show that although the erosion rate of BCSA was similar to portland cement, portland cement still had a slightly higher erosion resistance.
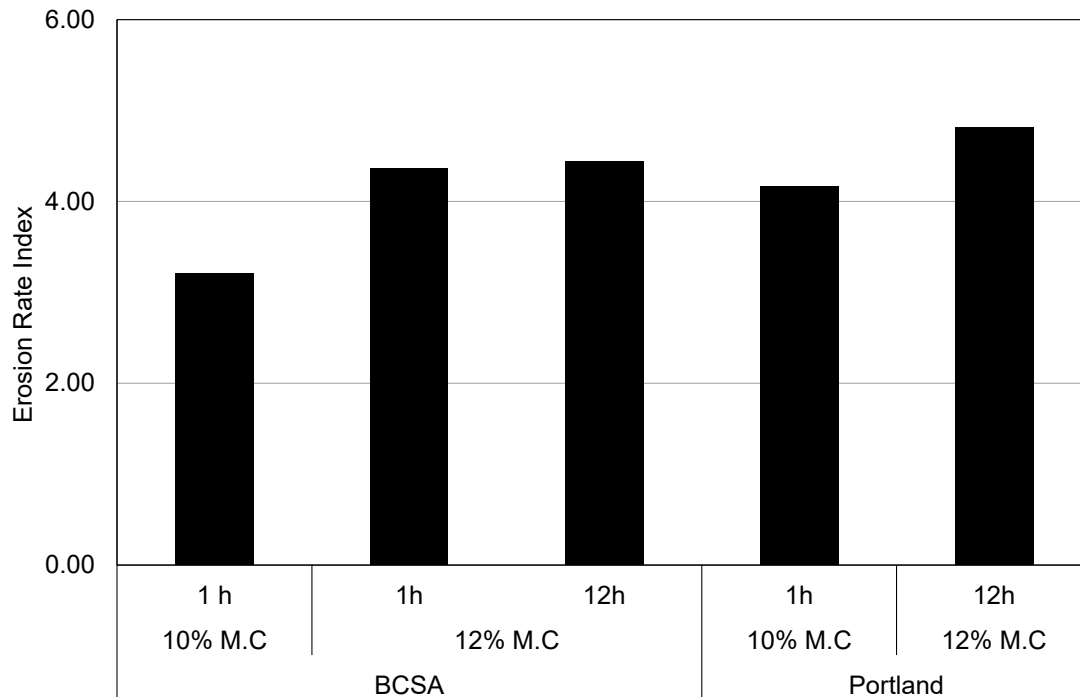

Figure 21. 70/30 soil-cement samples erosion performance, at 1 percent cement content.
Figure 22 presents the erosion performance of BCSA and portland cement samples with varying cement contents, all with a curing time of 1 hour and 10 percent MC. This figure shows that the erosion index for the soil-cement samples with 3 and 6 percent cement content had no detectible erosion. During these tests, no drop in differential pressure was observed and a maximum differential pressure of 19.90 psi was recorded. The final diameters differed from the initial ones by less than 0.04 in., measured using a caliper, so the highest possible value of the erosion rate index on the scale proposed by Wan and Fell (2002) was assigned. These samples will be tested using the pump system discussed in future research to try and quantify the onset of initial erosion.

When decreasing the cement content to 1 percent, erosion was detected in samples made with portland cement and BCSA cement. The sample made of portland cement had a higher erosion index when compared to the same mixture prepared with BCSA cement.
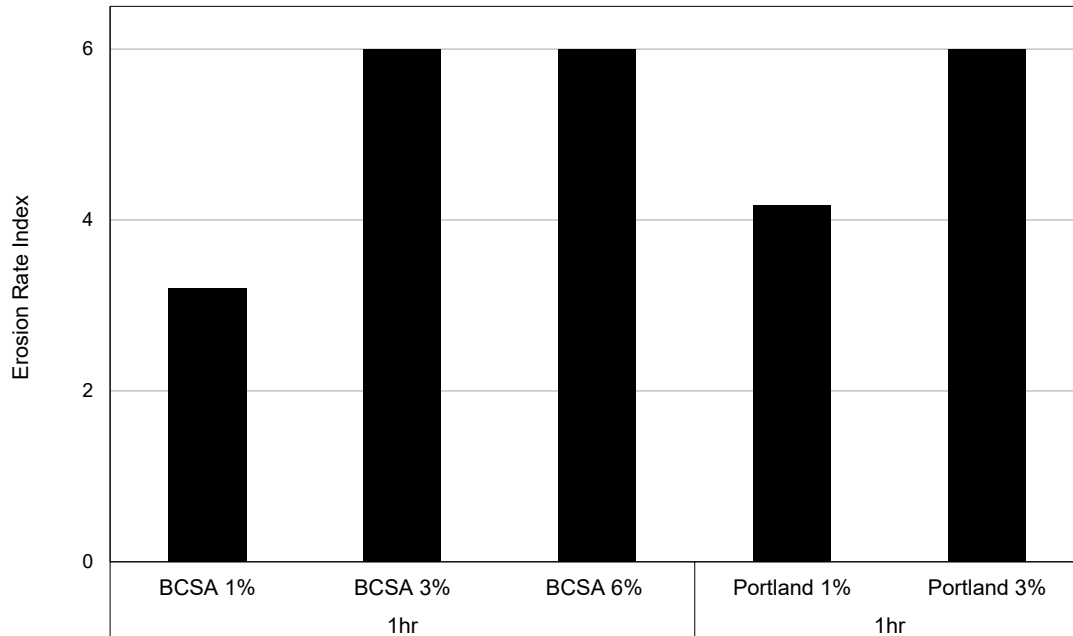

Figure 22. 70/30 Soil-cement samples erosion performance at various cement contents

An important takeaway from this research is that the control samples with no cement were difficult to run in the HET and exhibited high erodibility. Although not discussed herein, several combinations of soils were tested that had the hole collapse as the water levels were being initialized and essentially could not be tested. With only a small addition of 1 percent cement by weight, all of these soils could resist some erosion and remain stable. With 3 percent cement, these samples could not be eroded in the current setup and will need to be tested using the higher pressure pump system. Thus, the use of soil-cement as an erosion reduction measure and repair method is promising. More work is needed to further characterize the differences in BCSA and portland cement for early curing and the

relationship with water content. It is counter intuitive that portland cement would have a higher erosion resistance at 1 hour and additional tests are needed to better understand this occurrence. Testing the 3 and 6 percent samples at higher pressures and flow rates may show a different trend and help explain more of these findings.

IMPACTS/BENEFITS OF IMPLEMENTATION

The vulnerable condition of the country´s waterway systems and the magnitude of the repair costs to those structures as well as the high impact caused by the closures related to the problem is of high concern. One of the most recurring failures in embankments is internal erosion, which can be quite difficult to detect and repair. Therefore, BCSA soil-cement was tested to evaluate if it is a reasonable alternative for rapid repair and its potential to be used in flood fighting efforts. BCSA soil-cement is a promising alternative that performs similarly to portland cement when tested for erosion in cement contents of 3 and 6 percent by weight. Therefore, BCSA soil-cement can be used in active flooding efforts as a repair material for earthen structures and expect a similar performance against erosion as a typical portland soil-cement. No erosion was detected when either of these were exposed to water flow even at early curing ages of 1 hour. However, while 30 percent stronger than the companion portland cement mixture, BCSA soil-cement at 1 percent by weight, showed slightly worse erosion performance. The erosion performance of BCSA soil-cement could be augmented by changing its water content. Future experimental testing will explore this relationship as well as additional tests at higher pressures and flow rates to determine the onset of erosion for the 3 and 6 percent BCSA specimens. Overall, BCSA cement can be considered a good repair alternative thanks to the reduction in curing times and its ability to develop its strength faster.

CONCLUSIONS

This research investigated the use of BCSA soil-cement for rapid waterway repair applications. Unconfined compressive strength testing was performed and compared with control soil samples (no cement) and portland soil-cement samples. Additionally, HET was performed to compare the erodibility of the soil-cement mixtures. The conclusions from this study were as follows:

1. The average strengths for the tested BCSA soil-cement cylinders were significantly higher than the strengths from the previous MarTREC report, especially for those cylinders with a higher cement content. This improvement in the strength is attributed to a modification in the curing procedure used. This procedure consisted of storing the cylinders in sealed freezer bags instead of keeping the cylinders inside a moist cooler.

2. Samples prepared and compacted wet of the optimum moisture content led to the highest strengths for BCSA soil-cement. BCSA requires more water to hydrate which can explain the improved performance at higher moisture contents.

3. Without retarder, the mixture must be mixed and placed in less than 35 minutes. Additional time considerations will be needed to determine reasonable working times and implications in the field.

4. As the citric acid dosage was increased, the initial setting time increased linearly. The addition of 0.35 percent by cement weight of citric acid caused a delay of about 50 minutes in the peak hydration temperature. Citric acid seems to decrease the strength of mixtures even at later ages, but this effect seemed to be reduced as the cement content was reduced.

5. BCSA soil-cement cylinders with 3 and 6 percent cement contents successfully resisted erosion as early as 1 hour after addition of the cement. These samples could not be eroded in the current HET device.

6. Erosion could first be initiated in cylinders with 1 percent cement content, but even this small amount of cement showed improvement over the control samples.

7. For cylinders with 1 percent cement content, BCSA provided increased erosion resistance when the MC was slightly increased (from 10 percent to 12 percent). Therefore, it was determined that the erodibility of a soil is affected by the moisture content, even if the unconfined compressive strength was reduced.

Further Research

A zone of acceptance should be developed for BCSA soil-cement where the proportions can be specified to achieve adequate strength and erosion resistance. This would require balancing the cement content and MC of the soil-cement. In addition, it would be ideal to increase the number of tests performed and extend this work to other types of soils to determine if the observed effects are universal.

REFERENCES

[1]   J. Masters, "New report: U.S. dams, levees get D grades, need $115 billion in upgrades." [Online]. Available: New report: U.S. dams, levees get D grades, need $115 billion in upgrades

[2]   C. D. Murray, M. L. Barry, and A. J. Ortega Gonzalez, "Using CSA Cement for Novel Waterway Repair Materials," 2021.

[3]   A. J. Ortega Gonzalez, M. L. Bernhardt-Barry, and C. D. Murray, "Development of Underwater Mortar Using Belitic Calcium Sulfoaluminate Cement," *Adv Civ Eng Mater*, vol. 11, no. 1, p. 20210165, Aug. 2022, doi: 10.1520/ACEM20210165.

[4]   H. Afrin, "A Review on Different Types Soil Stabilization Techniques," *International Journal of Transportation Engineering and Technology*, vol. 3, no. 2, p. 19, 2017, doi: 10.11648/j.ijtet.20170302.12.

[5]   S. H. Carpenter, M. R. Crovetti, K. L. Smith, E. Rmeili, and T. Wilson, "SOIL AND BASE STABILIZATION AND ASSOCIATED DRAINAGE CONSIDERATIONS," 1992.

[6]   C. Jung and A. Bobet, "Post-Construction Evaluation of Lime-Treated Soils," 2008. doi: 10.5703/1288284313443.

[7]   C. McDowell, "Stabilization of Soils with Lime, Lime-Flyash, and Other Lime Reactive Materials," 1959.

[8]   S. Cement. ACI Committee 230 and American Concrete Institute., *Report on soil cement (ACI 230.1R-09)*. American Concrete Institute, 2009.

[9]   R. P. Bass, "QUALITY CONTROL OF SOIL-CEMENT CONSTRUCTION FOR WATER RESOURCES," 2000.

[10]   A. V. Da Fonseca, R. C. Cruz, and N. C. Consoli, "Strength properties of sandy soil-cement admixtures," *Geotechnical and Geological Engineering*, vol. 27, no. 6, pp. 681–686, Jan. 2009, doi: 10.1007/s10706-009-9267-y.

[11]   A. A. Firoozi, C. Guney Olgun, A. A. Firoozi, and M. S. Baghini, "Fundamentals of soil stabilization," *International Journal of Geo-Engineering*, vol. 8, no. 1, p. 26, 2017, doi: 10.1186/s40703-017-0064-9.

[12]   R. J. Schweizer and S. G. Wright, "A survey and evaluation of remedial measures for earth slope stabilization," 1974.

[13]   M. Shahandashti *et al.*, "Synthesis on Rapid Repair Methods for Embankment Slope Failure: Final Report Title: Synthesis on Rapid Repair Methods for Embankment Slope Failure," 2018. [Online]. Available: www.ntis.gov.

[14]   M. Jalili, R. Ghahroudi, M. Tajdini, K. Zadeh, and N. Zaeim, "Experimental Investigation of the Effective Parameters on the Strength of Soil-Cement," *Civil Engineering Infrastructures Journal*, vol. 53, no. 2, pp. 407–416, 2020, doi: 10.22059/ceij.2020.271426.1532.

[15]   W. B. Dinchak, "Soil-cement: it´s not just for highways anymore," 1989.

[16]   Portland Cement Association, "Soil-Cement Laboratory Handbook," 1992.

[17]   Das Braja M., *Geotechnical Engineering Handbook*. J. Ross Publishing, Inc., 2011. Accessed: Jul. 12, 2023. [Online]. Available:

https://app.knovel.com/hotlink/pdf/id:kt00C81372/geotechnical-engineering/lime-stabilization

[18]   Y.-K. Choi and K. D. Hansen, "RCC/Soil-Cement: What's the Difference?," 2005, doi: 10.1061/ASCE0899-1561200517:4371.

[19]   Portland Cement Association, "Suggested Specifications for Soil-Cement Base Course (SoilCement, Cement-Treated Base, Cement-Treated-Aggregate Base)," 2001.

[20]   Portland Cement Association, "Soil-cement Construction Handbook," 1995.

[21]   D. L. Richards and H. R. Hadley, "Soil-Cement Guide for Water Resources Applications," 2006. [Online]. Available: www.cement.org

[22]   K. D. Hansen, D. L. Richards, and M. E. Krebs, "PERFORMANCE OF FLOOD-TESTED SOIL-CEMENT PROTECTED LEVEES," 2011.

[23]   PCA, "Soil-cement laboratory handbook," 1999.

[24]   Portland Cement Association, "Soil-Cement (SC)." [Online]. Available: https://www.cement.org/cement-concrete/cement-specific-materials/soil-cement

[25]   S. Garber, R. O. Rasmussen, and D. Harrington, "Guide to Cement-Based Integrated Pavement Solutions," 2014.

[26]   R. P. Bass, "Hydraulic Structures-Designing with RCC and Soil-Cement," 2004.

[27]   E. Bescher, J. Stremfel, C. Ramseyer, and E. K. Rice, "The Role of Calcium Sulfoaluminate in Concrete Sustainability," 2012.

[28] C. A. J. D. de, W. E. P. L. M. N. M. L. O. & R. P. Hendriks, "Emission reduction of greenhouse gases from the cement industry," 1999.

[29] E. Bescher and John Kim, "Belitic Calcium Sulfoaluminate Cement: History, Chemistry, Performance, and Use in the United States Belitic calcium sulfoaluminate cement View project," 2019. [Online]. Available: https://www.researchgate.net/publication/334204807

[30] G. W. Cook and C. D. Murray, "Behavior of reinforced concrete made with belitic calcium sulfoaluminate cement at early ages," *ACI Mater J*, vol. 117, no. 1, pp. 167–174, 2020, doi: 10.14359/51719074.

[31] I. Chen, C. Hargis, and M. Juenger, "Understanding Expansion in Calcium Sulfoaluminate–Belite Cements," *Cem Concr Res*, vol. 42, pp. 51–60, Jan. 2012, doi: 10.1016/j.cemconres.2011.07.010.

[32] C. Acarturk, L. Burris, B. C. Acarturk, and L. E. Burris, "Effects of combination of retarders on calcium sulfoaluminate (CSA) cement systems Effects of combination of retarders on CSA cement systems," *International Conference on "Cement – Based Materials Tailored for a Sustainable Future,"* 2021, doi: 10.31224/osf.io/8ujyr.

[33] J. Pooni, D. Robert, F. Giustozzi, S. Setunge, Y. M. Xie, and J. Xia, "Novel use of calcium sulfoaluminate (CSA) cement for treating problematic soils," *Elsevier*, 2020.

[34] S. W. Moon, G. Vinoth, S. Subramanian, J. Kim, and T. Ku, "Effect of fine particles on strength and stiffness of cement treated sand," *Granul Matter*, vol. 22, no. 1, Feb. 2020, doi: 10.1007/s10035-019-0975-6.

[35] J. Purnomo, S. Sumarni, and I. N. Saputro, "Effect of citric acid on setting-time and compressive strength of concrete," in *IOP Conference Series: Materials Science and Engineering*, Institute of Physics Publishing, Oct. 2019. doi: 10.1088/1757-899X/578/1/012077.

[36] L. E. Burris and K. E. Kurtis, "Influence of set retarding admixtures on calcium sulfoaluminate cement hydration and property development," *Cement and Concrete Research Elsevier*, 2018.

[37] E. Soriano, "The Influence of Citric Acid on Setting Time and Temperature Behavior of Calcium Sulfoaluminate-Belite Cement," 2019.

[38] R. Tourment, B. Beullac, G. Degoutte, S. Patouillard, and J. Maurin, "Levees, Diversion Canals or Flood Expansion Areas?," 2007. doi: 10.1051/,6E3SWe bofConferencese3sconf/201FLOODrisk 2016 - 3rd European Conference on Flood Risk Management
7071200712007 (2016)© The Authors, published by EDP Sciences. This is an open access article distributed under the terms of the CreativeCommonsAttributi on License 4.0 (http://creativecommons.org/licenses/by/4.0/).

[39] ICOLD, "Statistical analysis of dam failures," 2019. Accessed: Nov. 01, 2023. [Online]. Available: https://www.icoldchile.cl/boletines/188.pdf

[40] M. Luthi, "A MODIFIED HOLE EROSION TEST (HET-P) TO STUDY EROSION CHARACTERISTICS OF SOIL," University of Applied Sciences Rapperswil, 2011.

[41] L. Zhang, Y. Xu, and J. S. Jia, "Analysis of earth dam failures: A database approach," *Georisk*, vol. 3, no. 3, pp. 184–189, Jan. 2009, doi: 10.1080/17499510902831759.

[42] Q. Zhong *et al.*, "Breaches of embankment and landslide dams - State of the art review," *Earth Sci Rev*, vol. 216, no. March, p. 103597, 2021, doi: 10.1016/j.earscirev.2021.103597.

[43] J.-L. B. I. S. H.-C. C. and Z. Medina-Cetina, *Relationship Between Erodibility and Properties of Soils*. 2019. doi: 10.17226/25470.

[44] J. L. Briaud, *Unsaturated and Saturated Soils*. 2013.

[45] Ohio Department of Natural Resources, "Dam Safety: Earth Dam Failures," 2019.

[46] Q. Zhong *et al.*, "Breaches of embankment and landslide dams - State of the art review," *Earth Sci Rev*, vol. 216, no. March, p. 103597, 2021, doi: 10.1016/j.earscirev.2021.103597.

[47] M. Luthi, "A MODIFIED HOLE EROSION TEST (HET-P) TO STUDY EROSION CHARACTERISTICS OF SOIL," University of Applied Sciences Rapperswil, 2011.

[48] C. F. Wan and R. Fell, "Investigation of Rate of Erosion of Soils in Embankment Dams," no. April, pp. 373–380, 2004.

[49] C. F. Wan and R. Fell, "Investigation of Internal Erosion and Piping of Soils in Embankment Dam." 2002.

[50] N. Benahmed and S. Bonelli, "Investigating concentrated leak erosion behaviour of cohesive soils by performing hole erosion tests," *European Journal of Environmental and Civil Engineering*, vol. 16, no. 1, pp. 43–58, 2012, doi: 10.1080/19648189.2012.667667.

[51]   R. Fell, C. Wan, J. Cyganiewicz, and M. Foster, "Time for Development of Internal Erosion and Piping in Embankment Dams," 2003, doi: 10.1061/ASCE1090-02412003129:4307.

[52]   ASTM, "Standard Practice for Thin-Walled Tube Sampling of Soils for Geotechnical Purposes," *ASTM Standard Practice*, vol. D1587-08, no. Reapproved 2007, pp. 1–4, 2008, doi: 10.1520/D1587-08R12E01.1.4.1.

[53]   J. Briaud *et al.*, "Erosion Function Apparatus for Scour Rate Predictions," vol. 5, no. February, pp. 105–113, 2001.

[54]   D. MAX SHEPPARD DAVID BLOOMQUIST and M. H. K. K. M. T. J. M. P. SLAGLE, "DESIGN AND CONSTRUCTION OF APPARATUS FOR MEASURING RATE OF WATER EROSION OF SEDIMENTS," Tallahassee, Florida, 2005.

[55]   T. Wahl, P.-L. Regazzoni, and Z. Erdogan, "Determining Erosion Indices of Cohesive Soils with the Hole Erosion Test and Jet Erosion Test Dam Safety Technology Development Program," no. October, 2008.

[56]   S. S. Lim, "Experimental investigation of erosion in variably saturated clay soils," 2006.

[57]   D. Marot, P.-L. Regazzoni, and T. Wahl, "Energy-Based Method for Providing Soil Surface Erodibility Rankings," *Journal of Geotechnical and Geoenvironmental Engineering*, vol. 137, no. 12, pp. 1290–1293, 2011, doi: 10.1061/(asce)gt.1943-5606.0000538.

[58]   N. Benahmed and S. Bonelli, "Investigating concentrated leak erosion behaviour of cohesive soils by performing hole erosion tests," *European Journal of Environmental*

and Civil Engineering, vol. 16, no. 1, pp. 43–58, 2012, doi: 10.1080/19648189.2012.667667.

[59] I. Haghighi, C. Chevalier, M. Duc, S. Guédon, and P. Reiffsteck, "Improvement of Hole Erosion Test and Results on Reference Soils," *Journal of Geotechnical and Geoenvironmental Engineering*, vol. 139, no. 2, pp. 330–339, 2013, doi: 10.1061/(asce)gt.1943-5606.0000747.

[60] L. Xie, X. Liang, and T. C. Su, "Measurement of pressure in viewable hole erosion test," *Canadian Geotechnical Journal*, vol. 55, no. 10, pp. 1502–1509, 2018, doi: 10.1139/cgj-2017-0292.

[61] M. J. Bora, W. Cai, S. Pekkat, A. Garg, and S. Sekharan, "Development of a simplified theoretical model to determine erodibility of compacted soil in hole erosion test based on fluid energy transformation," *Acta Geotech*, vol. 18, no. 10, pp. 5441–5455, 2023, doi: 10.1007/s11440-023-01877-6.

[62] B. Zaid, F. Vollert, J. Gibmeier, L. Mengel, O. Stelzer, and A. Schneider, "Application of micro-computed X-ray tomography for improving the hole erosion test analysis on high plastic clay," *Acta Geotech*, vol. 18, no. 2, pp. 865–876, 2022, doi: 10.1007/s11440-022-01606-5.

[63] ASTM D698-12, *Standard Test Methods for Laboratory Compaction Characteristics of Soil Using Standard Effort*. 2021.

[64] ASTM, "Standard Test Methods for Laboratory Compaction Characteristics of Soil Using Standard Effort (12,400 ft-lbf/ft 3 (600 kN-m/m 3)) 1," 2021, doi: 10.1520/D0698-12R21.

[65]   ASTM D2166-06, *Standard Test Method for Unconfined Compressive Strength of Cohesive Soil*. 2010.

[66]   N. Moragoda, M. Kumar, and S. Cohen, "Representing the role of soil moisture on erosion resistance in sediment models: Challenges and opportunities," *Earth Sci Rev*, vol. 229, no. January, p. 104032, 2022, doi: 10.1016/j.earscirev.2022.104032.